Atmos. Meas. Tech. Discuss., doi:10.5194/amt-2016-49, 2016
Manuscript under review for journal Atmos. Meas. Tech.
Published: 7 March 2016

Atmospheric Measurement Techniques Discussions

Toward autonomous surface-based infrared remote sensing of polar clouds: Cloud height retrievals

Penny M. Rowe[1,2], Christopher J. Cox[3,4], and Von P. Walden[5]

[1]NorthWest Research Associates, Redmond, WA, USA
[2]Physics Department, Universidad de Santiago de Chile, Santiago, Chile
[3]Cooperative Institute for Research in Environmental Sciences, University of Colorado, Boulder, CO, USA
[4]NOAA Earth System Research Laboratory, Physical Sciences Division, Boulder, CO, USA
[5]Department of Civil and Environmental Engineering, Washington State University, Pullman, WA, USA

Correspondence to: Penny M. Rowe (penny@nwra.com)

Abstract. Polar regions are characterized by their remoteness, making measurements challenging, but an improved knowledge of clouds and radiation is necessary to understand polar climate change. Infrared radiance spectrometers can operate continuously from the surface and have low power requirements relative to active sensors. Here we explore the feasibility of retrieving cloud height with an infrared spectrometer that would be designed for use in remote locations, for single-layer, mixed-phase polar clouds, using the CO_2 slicing/sorting and the Minimum Local Emissivity Variance (MLEV) methods. In the absence of imposed errors and for clouds with optical depths greater than ∼0.3, cloud height retrievals from simulated spectra using CO_2 slicing/sorting and MLEV are found to have roughly equivalent, high accuracies: at an instrument resolution of 0.5 cm^{-1}, mean biases are found to be ∼0.2 km for low clouds (bases below 2 km) and -0.2 km for medium-to-high clouds (hereafter "high clouds"). Accuracy is found to decrease with decreasing cloud signal and increasing cloud height (independent of signal). Accuracy also decreases with coarsening resolution and becomes worse overall for MLEV than for CO_2 slicing/sorting; however, the two methods have differing sensitivity to different sources of error, suggesting an approach that combines them. In the presence of errors, the dependence of retrieval accuracy on resolution is weakened. Further, errors have a small effect on retrievals of low clouds but a large effect on high clouds. Expected errors in the atmospheric state indicate that at a resolution of 0.5 cm^{-1}, instrument noise level and bias of 0.1 mW/(m^2 sr cm^{-1}) would permit a retrieval accuracy of -2 ± 2 km for high clouds and ∼0.2 ± 0.5 km for low clouds, for both methods. This study highlights the sensitivity of surface-based infrared spectrometers to low clouds prevalent in polar regions.

1 Introduction

The interactions between clouds and radiation are important drivers of variability in the climate system. At high latitudes, unique processes are at work, with important implications for climate. For example, in the Arctic, the solar and infrared effects of clouds influence interannual variability in sea ice through modulation of the ice-albedo, water vapor, and cloud feedbacks (Choi et al., 2014; Francis and Hunter, 2007; Kay et al., 2008; Schweiger et al., 2008a, b). Cloud heights may be changing in the Arctic in response to changes in sea ice (Francis and Hunter, 2007; Schweiger et al., 2008a), thereby modifying the

Atmos. Meas. Tech. Discuss., doi:10.5194/amt-2016-49, 2016
Manuscript under review for journal Atmos. Meas. Tech.
Published: 7 March 2016

Atmospheric Measurement Techniques Discussions

surface energy budget and perturbing feedbacks. In the Antarctic, clouds have large impacts on ice/snow mass balance and the heat and freshwater budgets of the Southern Ocean, which in turn affect global ocean circulation and the global carbon cycle (Bromwich et al., 2012). These impacts highlight the importance of understanding responses of clouds to changes in the system. Measurements of cloud properties with high spatial and temporal resolution are critical for this work, but currently data is sparse at high latitudes.

Measurements of cloud properties are also needed to validate models of the Arctic and Antarctic atmospheres and to improve the parameterizations they rely on (Hines et al., 2004; Town et al., 2007; Wesslen et al., 2014). Large errors in atmospheric radiative fluxes and cloud radiative forcing are found in reanalysis products (Walsh et al., 2009; Cox et al., 2012; Wesslen et al., 2014) and climate models (Cesana and Chepfer, 2013; Pithan and Mauritsen, 2014; Pithan et al., 2014). These errors have been attributed to errors in optical properties, vertical profiles, and cloud base heights in the Arctic (Walsh et al., 2009). Cloud height, which influences cloud temperature, has a large impact on the cloud infrared radiation and thermodynamic phase; Wesslen et al. (2014) find that ERA-Interim cloud base height is often too high in the Arctic. Spatially resolved measurements of cloud properties at high latitudes come primarily from satellite platforms (e.g., Francis and Hunter, 2007; Schweiger et al., 2008a; Wang and Key, 2003, 2005). Active instruments, such as CloudSat and the Cloud-Aerosol Lidar and Infrared Pathfinder Satellite Observation (CALIPSO) allow retrievals of cloud height and other properties (see, e.g. Bromwich et al., 2012; Cesana et al., 2012; Verlinden et al., 2011). However, lidar instruments have a small footprint, requiring the use of monthly or seasonal averaging. Passive instruments that measure upwelling infrared radiances (e.g. the Moderate Resolution Imaging Spectroradiometer (MODIS), the Infrared Interferometer Spectrometer (IRIS), the Infrared Atmospheric Sounding Interferometer (IASI), and the Crosstrack Infrared Sounder (CrIS)) have large footprints, enabling global coverage on daily timescales, and can be used to retrieve cloud properties. These instruments have the advantage that the cloud property retrievals are derived from, and are thus directly tied to, their radiative effect. However, passive instruments aboard satellite platforms are best suited for viewing the tops of clouds and have less sensitivity to the important region of the atmosphere that affects the surface energy budget, that is, between the surface and the base of the cloud. Because of this, satellite-based measurements must be complemented by surface-based measurements for a complete understanding of the atmosphere.

Atmospheric observatories that are capable of surface-based remote sensing of cloud properties exist in the Arctic at a small number of coastal and interior land stations, most notably Barrow, Alaska (Stamnes et al., 1999), Eureka, Canada, Ny-Ålesund, Svalbard and Summit, Greenland (Shupe et al., 2013). In addition, a number of brief field campaigns with similar capabilities have been conducted over the Arctic Ocean, including the Surface Heat Budget of the Arctic (SHEBA) campaign (Uttal et al., 2002), the Mixed-Phase Arctic Cloud Experiment (MPACE; Verlinde et al., 2007), the Arctic Summer Cloud Ocean Study (ASCOS; Wesslen et al., 2014), and the Norwegian Young Sea Ice (N-ICE) experiment. In the Antarctic, field stations are sparsely located, principally on the coast, and have fewer instruments for measuring cloud properties than in the Arctic. The ARM mobile facility (AMF) is deploying in McMurdo for a year from November 2015 to 2017 and long-term lidar measurements are made at Amundsen-Scott South Pole Station. Nevertheless, there remains a dearth of surface-based remote sensors in the Antarctic. The lack of instrumentation at both poles is due largely to the expense and logistical challenge of deploying instruments in these remote regions. A lack of autonomous sensors prevents collection of data at locations other than

Atmos. Meas. Tech. Discuss., doi:10.5194/amt-2016-49, 2016
Manuscript under review for journal Atmos. Meas. Tech.
Published: 7 March 2016

Atmospheric Measurement Techniques Discussions

established stations. New instruments are needed that address these challenges, in particular designs intended for the purposes of both climate monitoring and process studies representing a more comprehensive range of regional high-latitude climates.

Surface-based Fourier transform infrared (FTIR) spectrometers are proven instruments both in the Antarctic (e.g. Mahesh et al., 2001a, b; Rowe et al., 2008) and the Arctic (e.g. Rathke et al., 2002; Mariani et al., 2013; Cox et al., 2014). Cloud height is required to determine cloud temperature or retrieve cloud optical and microphysical properties. Surface-based FTIR spectrometers are currently operated at large, well-instrumented observatories, and therefore retrievals of cloud properties from downwelling radiances typically do not include cloud height, but rather use cloud height measured by collocated lidars. However, a legacy of stand-alone passive infrared remote sensors have resulted in developments of methods for retrieving cloud height primarily from satellite instruments measuring infrared radiances (e.g. Smith and Platt, 1978; Minnis et al., 2001; Kahn et al., 2007), but also a few ground-based studies using downwelling infrared radiances (Mahesh et al., 2001a). FTIR technology is passive and can be relatively low-cost, with energy requirements that are considerably lower than active instrumentation such as lidar (e.g. Christensen et al., 2004). Furthermore, passive infrared measurements are well-suited for observing clouds in dry climates such as the polar regions (Mahesh et al., 2001a; Neshyba and Rathke, 2003; Cox et al., 2014). Thus, portable, autonomous infrared spectrometers are a viable solution for acquiring long-term, high temporal resolution, surface-based measurements of clouds and the atmospheric state from a more spatially diverse and comprehensive sample of the high latitudes. Since such an autonomous system would necessitate independence from other collocated, ancillary measurements, such as lidar, evaluating the requirements for accurate cloud height retrievals is a first step towards development of such a system.

Here we evaluate the potential for using infrared spectrometers for retrieving cloud base height, specifically testing the uncertainties associated with instrument designs suited for autonomous deployment. In particular, noise characteristics depend on instrument resolution (which limits the instrument throughput), and hence noise decreases as resolution becomes coarser. Thus we also test the effects of instrument resolution on the accuracy of cloud height retrievals. To isolate uncertainties associated with methodology and instrument characteristics, our analysis makes use of a simulated data set (Cox et al., 2016) that permits control over sources of error and maintains a fixed and known standard for comparison. Three established methods for retrieving cloud height using spectrally-resolved infrared instruments are the minimum local emissivity variance (MLEV) technique (Huang et al., 2004), CO_2 slicing (e.g. Menzel et al., 1983; Mahesh et al., 2001a) and CO_2 slicing/sorting (Holz et al., 2006). Although these have been compared for satellite-based retrievals from upwelling radiances (Holz et al., 2006), they have not been compared for retrievals from downwelling radiances or with consideration of variability in noise-characteristics and spectral sampling between different types of spectrometers, which are key engineering barriers to developing an autonomous surface-based system. Here we evaluate and compare these techniques to determine which is most accurate for surface-based retrievals of downwelling radiance in the Arctic and to constrain the instrument requirements for providing cloud height information from an infrared spectrometer that is designed for autonomous deployment.

Atmos. Meas. Tech. Discuss., doi:10.5194/amt-2016-49, 2016
Manuscript under review for journal Atmos. Meas. Tech.
Published: 7 March 2016

Atmospheric Measurement Techniques Discussions

2 Atmospheric State and Simulated Radiances

In order to assess the cloud height retrievals, simulated cloudy-sky radiances are used. A wide variety of simulations were created, described in detail by Cox et al. (2016, submitted), and summarized here. Line-by-line, or perfect resolution spectra were created for a spectral range of 50 to 3000 cm^{-1} (spectra in the range 500 to 950 cm^{-1} are used in this work), using the Line by Line Radiative Transfer Model (LBLRTM); (Clough et al., 2005) and the DIScrete Ordinates Radiative Transfer (DISORT) model (Stamnes et al., 1988). This dataset is designed to be of use for feasibility studies of retrievals such as the present study. The simulated dataset allows tests of retrieval accuracy to focus on a few variables, while constraining others. To this end, the cloud and atmosphere modeling was simplistic: only single-layer clouds were included and a plane-parallel atmosphere was assumed. Furthermore, cases with ice modeled as spheres are used here, and all clouds are vertically homogenous. This allows the study to focus on retrieval accuracy with varying atmospheric profiles, precipitable water vapor amounts as well as varying cloud heights, temperatures, optical depths, ice fractions, and effective radii. A variety of typical Arctic atmospheres are represented in the data set, including conditions for all four seasons and a variety of cloud types. Because of the high incidence of mixed phase clouds in polar regions, both single phase and mixed phase clouds were included (mixed phase clouds were modeled as externally mixed).

Cloud base heights range from 0 to 7 km with temperatures ranging from 225 to 283 K. Figure 1, reproduced from Cox et al. (2016), shows the distributions of cloud height, thickness, and temperature. To test the limits of cloud property retrievals, a few extreme and/or less likely cases were included. For example, the database includes a few cases of clouds with optical depths that are extremely low (visible optical depths below 0.2) and includes high clouds that are optically thick as well as thin. Precipitable water vapor (PWV) amounts span the range typical of the polar regions, but some cases are included that are quite high for the polar regions (mean = 1 cm, standard deviation = 0.72 cm, maximum = 3 cm, minimum = 0.2 cm). Overall most of the atmospheric and cloud properties in the model are intended to be realistic cases and, therefore, good candidates for cloud height retrievals. Additionally, the distributions are intended to be realistic for the Arctic; cloud heights are typically low with fewer high clouds.

The perfect resolution spectra were convolved with sinc functions to create sets of simulated cloudy-sky radiances at resolutions of 0.1, 0.5, 1, 2, 4, and 8 cm^{-1}. These simulated cloudy-sky radiances serve as the "observations", R_{obs}, used to test the cloud height retrievals.

3 Cloud height retrieval methods

In this section we introduce the established methods for retrieving cloud height from infrared radiances: the minimum local emissivity variance (MLEV) technique (Huang et al., 2004) and CO_2 slicing (e.g. Smith and Platt, 1978; Mahesh et al., 2001a; Holz et al., 2006) and then expand upon these by developing hybrid methodologies suitable for surface-based observations of downwelling radiances in polar regions. We first derive the radiative transfer equations central to the methodological theory. (The derivation is similar to but differs slightly in symbols and development from those of Mahesh et al. (2001a), Holz et al. (2006), and Huang et al. (2004) in order to illustrate some key points.) Next we describe MLEV, followed by the CO_2 slicing

Atmos. Meas. Tech. Discuss., doi:10.5194/amt-2016-49, 2016
Manuscript under review for journal Atmos. Meas. Tech.
Published: 7 March 2016

Atmospheric Measurement Techniques Discussions

method as applied by Mahesh et al. (2001a) and the CO_2 slicing/sorting method of Holz et al. (2006). MLEV and CO_2 slicing typically use radiances from within 710 to 950 cm^{-1} and ignore scattering. Holz et al. (2006) implement the CO_2 slicing differently than Mahesh et al. and also introduce "CO_2 sorting," whereby wavenumbers are selected after sorting them roughly according to their atmospheric transmittance. Finally, we describe modifications made to the MLEV and CO_2 slicing and sorting methods made in this work. For MLEV, the method is modified for downwelling radiances, while for CO_2 slicing and sorting, the best aspects of the methods of Holz et al. (2006) and Mahesh et al. (2001a) are combined, based on experimentation with retrievals from the dataset of simulated Arctic downwelling radiances. The retrievals all assume a zenith view.

3.1 Cloud Emissivity

Both MLEV and CO_2 slicing depend on approximations involving the cloud emissivity over the wavenumber range of interest: MLEV assumes it is smoothly-varying with wavenumber, while CO_2 slicing traditionally assumes it is constant. Ignoring scattering, the observed downwelling radiance for a zenith view, R_{obs}, is

$$R_{\text{obs}} \approx \int_0^{\text{TOA}} B(T(z)) \frac{dt}{dz} dz, \tag{1}$$

where the parentheses represent functionality, B is the Planck function, T is temperature, z is height, t is the transmittance from the surface to z, and the integration is from the surface (height of 0) to the top of atmosphere (TOA). The integral can be broken up into contributions from the surface to the cloud base (base), from cloud base to cloud top (top), and from cloud top to the TOA. The radiance contribution from the surface to the cloud base (R_c) is unaffected by the presence of the cloud.

$$R_{\text{obs}} \approx R_c + \int_{\text{base}}^{\text{top}} B(T(z)) \frac{dt}{dz} dz + \int_{\text{top}}^{\text{TOA}} B(T(z)) \frac{dt}{dz} dz. \tag{2}$$

If we assume that the cloud is in an infinitely thin layer ($z_{base} = z_{\text{top}}$) devoid of gases (i.e. gaseous transmittance within the cloud equals unity), a number of simplifications are possible. We let $B(T(z_{base})) = B(T(z_{\text{top}})) = B_c$, the Planck function at the cloud temperature. The first integral on the right hand side can then be solved to give $B_c[1 - t_{cld}]t_c$ where t_c is the gaseous transmittance from the surface to the cloud base and t_{cld} is the cloud transmittance. We have

$$R_{\text{obs}} \approx R_c + B_c t_c [1 - t_{cld}] + t_{cld} \int_{\text{top}}^{\text{TOA}} B(T(z)) \frac{dt'}{dz} dz \tag{3}$$

where t' is the cloud-free transmittance from the surface to height z. The final integral is the radiance contribution from above the cloud that makes it through the gaseous atmosphere below the cloud; it is independent of the cloud presence and is equal to $R_{\text{clr}} - R_c$. Assuming local thermodynamic equilibrium (and again ignoring scattering), the cloud absorptivity equals the emissivity, so that $(1 - t_{cld}) = \epsilon$. We can ignore the cloud fraction if the instrument field of view is small, but the emissivity can also be thought of as an effective emissivity that takes into account any patchiness in the cloud within the field of view.

$$R_{\text{obs}} \approx R_c + \epsilon B_c t_c + [R_{\text{clr}} - R_c] t_{cld}. \tag{4}$$

Atmos. Meas. Tech. Discuss., doi:10.5194/amt-2016-49, 2016
Manuscript under review for journal Atmos. Meas. Tech.
Published: 7 March 2016

Atmospheric Measurement Techniques Discussions

Substituting in (1 - ϵ) for t_{cld} and simplifying gives

$$R_{\text{obs}} \approx R_{\text{clr}} + \epsilon[B_c t_c + R_c - R_{\text{clr}}]. \tag{5}$$

The equation can be rearranged to solve for the emissivity,

$$\epsilon \approx \frac{R_{\text{obs}} - R_{\text{clr}}}{B_c t_c + R_c - R_{\text{clr}}}. \tag{6}$$

Eq. (6) is comparable to Eq. (4) of Huang et al. (2004) and Eq. (2) of Holz et al. (2006), where $R_{\text{cld}} = B_c t_c + R_c$. The equation in the form shown here demonstrates that cloud height and effective emissivity are very closely connected, making cloud height retrievals challenging. B_c depends on cloud temperature, which in turn depends on cloud height, and t_c and R_c both depend on cloud height. Thus errors in cloud height can be largely accounted for by errors in emissivity.

The right hand side of Eq. (6) depends on the observed radiance, R_{obs}, and quantities that can be calculated based on knowledge of the cloud-free atmospheric state. In this work, R_{clr} and R_c are calculated from atmospheric profiles of height, pressure, temperature, and trace gas amounts, using radiative transfer calculations as in the line by line radiative transfer model (LBLRTM; Clough et al., 1992). R_{clr} need only be calculated once, whereas t_c and R_c are calculated for each potential cloud height. R_{clr}, t_c and R_c all include gaseous contributions and therefore vary rapidly with frequency. By contrast, ϵ and B_c depend on the cloud properties and should vary slowly with frequency.

To summarize the model assumptions, they include modeling the atmosphere as a plane-parallel, layered atmosphere in local thermodynamic equilibrium, ignoring scattering, assuming the cloud is in an infinitesimally thin layer devoid of gases, and assuming that the emissivity is slowly-varying or constant with frequency over ~710-950 cm^{-1}.

3.2 MLEV

To find the MLEV, ϵ is calculated for each potential cloud height, c, for wavenumbers between limits ν_1 and ν_2. The "local" emissivity variance (LEV) is then calculated according to Eq. (5) of Huang et al. (2004),

$$LEV_c = \sum_{\nu_1}^{\nu_2} (\epsilon_{c,\nu} - \langle \epsilon_{c,\nu} \rangle)^2, \tag{7}$$

where this is defined as the local emissivity variance because the mean of ϵ is not taken over the entire spectral range ν_1 to ν_2, but rather over a small wavenumber region ($\Delta\nu$) about ν,

$$\langle \epsilon(c,\nu) \rangle = \frac{1}{\Delta\nu} \sum_{\nu-\Delta\nu/2}^{\nu+\Delta\nu/2} \epsilon_{c,\nu}, \tag{8}$$

The summation in Eq. (7) is over a wavenumber range that includes water vapor and CO_2 lines. Huang et al. (2004) use ν_1 = 750 cm^{-1} and ν_2 = 950 cm^{-1} in Eq. (7) and use an interval of $\Delta\nu$ = 5 cm^{-1} in Eq. (8). When Eq. (7) is calculated with an incorrect height, errors in the calculated values of t_c and R_c result in errors in the calculated effective emissivity that vary rapidly with frequency due to the dependence of t_c and R_c on trace gases, causing the LEV to be large. Thus the correct

Atmos. Meas. Tech. Discuss., doi:10.5194/amt-2016-49, 2016
Manuscript under review for journal Atmos. Meas. Tech.
Published: 7 March 2016

Atmospheric Measurement Techniques Discussions

cloud height is retrieved as that corresponding to the minimum LEV, or MLEV. This technique relies on accurate knowledge of carbon dioxide and water vapor profiles; uncertainties in the water vapor profile are thus an importance source of error.

In this work, the MLEV method is performed similarly to that of Huang et al. (2004), but for downwelling radiances and for a variety of different spectral resolutions. Furthermore, all values are calculated for the desired instrument resolution. This is done by convolving $R_{\rm clr}$, t_c, and R_c with a sinc funciton with the desired linewidth. As in Huang et al. (2004), we use ν_1 = 750 and ν_2 = 950 cm^{-1}. For resolutions of 0.5 and 1 cm^{-1}, we use an interval of $\Delta\nu = 5$ cm^{-1} in Eq. (8) (corresponding to averaging over 10 or 5 spectral points, respectively), like Huang et al. (2004). However, for a resolution of 2 cm^{-1}, we use $\Delta\nu = 10$ cm^{-1} (average over 5 points), and for resolutions of 4 and 8 cm^{-1}, we use $\Delta\nu = 24$ cm^{-1} (average over 6 or 3 points, respectively). Small variations about these values were found to give similar results.

The steps for MLEV are as follows:

1. Choose model heights (layer boundaries) for the model atmosphere. Calculate $R_{\rm clr}$. Calculate R_c, B_c, and t_c for each model height for the clear-sky atmosphere based on best estimates of temperature, water vapor, and trace gas amounts.
2. Calculate the LEV (Eq. (6) - Eq. (8)) for each trial cloud height.
3. Find the height that corresponds to the MLEV.

3.3 CO_2 slicing and sorting

In Mahesh et al. (2001a), CO_2 slicing makes use of the variation in the absorption coefficient of the CO_2 band from $\sim$ 700 to 755 cm^{-1}, where CO_2 emission dominates. (Unlike H_2O, CO_2 is a well-mixed gas and thus can be estimated fairly accurately from surface measurements.) Rearranging Eq. (5), including the wavenumber dependence explicitly, and dividing both sides by the same quantities at a reference wavenumber, ν_0, gives

$$\frac{R_{\rm obs}(\nu) - R_{\rm clr}(\nu)}{R_{\rm obs}(\nu_0) - R_{\rm clr}(\nu_0)} = \frac{\epsilon(\nu)[B_c(\nu)t_c(\nu) + R_c(\nu) - R_{\rm clr}(\nu)]}{\epsilon(\nu_0)[B_c(\nu_0)t_c(\nu_0) + R_c(\nu_0) - R_{\rm clr}(\nu_0)]}. \quad (9)$$

The value of ν is varied from $\sim$ 700 to 755 cm^{-1}, while ν_0 is chosen to be a wavenumber ($\sim$ 812 cm^{-1}) close to this spectral region but where the absorption coefficient of CO_2 is small enough (i.e. the transmittance is large enough) that the downwelling radiance is sensitive to the entire atmospheric column. It is next assumed that the emissivity is constant from 700 to 812 cm^{-1}, so that the emissivity terms cancel.

$$\frac{R_{\rm obs}(\nu) - R_{\rm clr}(\nu)}{R_{\rm obs}(\nu_0) - R_{\rm clr}(\nu_0)} = \frac{B_c(\nu)t_c(\nu) + R_c(\nu) - R_{\rm clr}(\nu)}{B_c(\nu_0)t_c(\nu_0) + R_c(\nu_0) - R_{\rm clr}(\nu_0)}. \quad (10)$$

The left hand side (LHS) of Eq. (10) is constant, while the right hand side (RHS) varies with assumed cloud height. Solutions are found at each wavenumber where the RHS equals the LHS, giving a retrieved cloud height for each ν. If the RHS is not equal to the LHS at any height, the solution is found where the magnitude of the difference (RHS-LHS) is smallest. Due to model and measurement errors, retrieved cloud heights vary for different values of ν. (Note that Mahesh et al. retrieve cloud base pressure, rather than height; in this work, cloud base height is retrieved). Mahesh et al. take a weighted average of the

Atmos. Meas. Tech. Discuss., doi:10.5194/amt-2016-49, 2016
Manuscript under review for journal Atmos. Meas. Tech.
Published: 7 March 2016

Atmospheric Measurement Techniques Discussions

results obtained, where the weights are the change in the RHS with a change in the pressure at the cloud base, determined in a 10 hPa interval centered about the retrieved cloud base pressure. This typically provides more weight to wavenumbers with "e-folding" distances close to the cloud base.

Multiple solutions may exist at a given ν due to errors or due to the presence of near-surface temperature inversions, which are common in the polar regions. Due to a temperature inversion, the cloud temperature may exist at more than one height. Because the retrieval methodology relies to a large extent on sensitivity to cloud temperature (rather than height), choosing between heights having the same temperature can be challenging. To do this, the best result is determined for each set of solutions (e.g. the set below the inversion and the set above the inversion). Then, to choose between sets of cloud bases above and below a temperature inversion, Mahesh et al. perform a second step using "short-sighted" wavenumbers. Short-sighted wavenumbers are those with low transmittances, and are sensitive to low clouds but not high clouds. Mahesh et al. find the percentage of short-sighted wavenumbers at which a cloud is detected. If this is large, the cloud base is assumed to be within the inversion, and if it is small, the cloud base is assumed to be above the inversion.

The CO_2 slicing/sorting method of Holz et al. (2006) refines the CO_2 slicing technique by selecting a subset of wavenumbers within 650 to 800 cm^{-1} to use for the retrieval. Wavenumbers are sorted roughly according to the gaseous transmittance. For downwelling radiances, the transmittance is defined from the surface up to some level in the atmosphere. As the transmittance increases with (sorted) wavenumber, the effective emitting height becomes higher. Holz et al. (2006) use clear-sky brightness temperature as a proxy for clear-sky transmittance. (As will be discussed, this is a reasonable proxy if temperatures decrease with height in the troposphere, which is not always the case for this work.) First, clear-sky brightness temperatures are sorted. The sorted index is then applied to cloudy-sky brightness temperatures. Sorted clear-sky and cloudy-sky brightness temperatures are then compared to determine at which wavenumbers they differ. Sorted wavenumbers are only used in the retrieval if the clear-sky and cloudy-sky brightness temperatures differ. This sets the lower limit in the gaseous transmittance such that wavenumbers that have little sensitivity to the cloud are excluded from the cloud height determination. An upper limit in gaseous transmittance is also selected, based on where the slope of the brightness temperature decreases. Finally, Holz et al. found results were improved if only wavenumbers between strong CO_2 absorption lines were used.

Once the subset of wavenumbers to be used has been determined, a unique cloud height is determined for each wavenumber in a similar manner as for CO_2 slicing, but using a different formulation, which is designed for upwelling radiances (see Eq. (1) of Holz et al. (Holz et al., 2006)).

After a unique cloud height has been found for each wavenumber, the method for determining the best overall cloud height also differs from that of Mahesh et al. (2001a). Instead of weighting the cloud heights, an error function is computed for each retrieved cloud height, c.

$$Err = \sum_{\nu'} R_{\text{obs}}(\nu) - R_{\text{clr}}(\nu) - \epsilon_c(\nu_0)[B_c(\nu)t_c(\nu) + R_c(\nu) - R_{\text{clr}}(\nu)]. \tag{11}$$

The sum is over the selected wavenumbers, ν'. The optimal cloud height is chosen as that which minimizes this equation.

This work uses aspects of the CO_2 slicing method of Mahesh et al. as well as the CO_2 slicing/sorting method of Holz et al. (2006) and additional adaptations for computational efficiency and for cloud retrievals specifically from downwelling radiance

Atmos. Meas. Tech. Discuss., doi:10.5194/amt-2016-49, 2016
Manuscript under review for journal Atmos. Meas. Tech.
Published: 7 March 2016

Atmospheric Measurement Techniques Discussions

measurements made in the polar regions. Based on detailed sensitivity studies and trial-and-error, the following modifications were made.

CO_2 sorting is applied slightly differently in this work. The use of brightness temperature as a proxy for transmittance, as in Holz et al. (2006), is not a good approximation in the polar regions. While gaseous transmittance, which is defined relative to the surface, always decreases with height, clear-sky brightness temperatures do not always decrease with height in the polar regions; they can increase with height within near-surface temperature inversions, which are common in the polar regions. Thus in our method, wavenumbers are sorted by gaseous transmittance from the surface to the TOA, t_{TOA}. The gaseous transmittances are calculated for each measured radiance spectrum (at the desired resolution) based on the clear-sky atmospheric state and then sorted.

Another difference in our application of sorting involves setting the threshold for choosing the wavenumbers to use. Within the spectral range of 700 to 750 cm^{-1}, at some wavenumbers CO_2 transmits so little radiance that there is little sensitivity to cloud. At these wavenumbers, $R_{\mathrm{obs}} - R_{\mathrm{clr}}$ is expected to be on the order of the uncertainty. Thus a threshold is needed for which there is adequate cloud signal for the retrieval. A threshold of 0.5 RU is used here (1 RU, or radiance unit, is defined to be 1 mW / [m^2 sr cm^{-1}]). The gaseous transmittance t_{thresh} is found at which the magnitude of $R_{\mathrm{obs}} - R_{\mathrm{clr}} = 0.5$ RU, and wavenumbers (ν) are selected that correspond to $t_{\mathrm{TOA}} \geq t_{\mathrm{thresh}}$. A final difference is that an upper wavenumber cutoff of 755 cm^{-1} is used, rather than estimating a cut-off based on the slope of the brightness temperature; the retrieval is not sensitive to the choice of upper wavenumber.

Like Mahesh et al., we use short-sighted wavenumbers to distinguish between multiple solutions. However, whereas Mahesh et al. found that wavenumbers between 670 and 700 cm^{-1} are sensitive to clouds within the inversion, this wavenumber range was found to have negligible sensitivity to clouds at any height for the atmospheric profiles used here. Instead, the best wavenumber range for the atmospheric profiles used here is found to be 705 to 715 cm^{-1}. In addition, sensitivity studies indicate that a better method than that employed by Mahesh et al. is to once more find the solution that minimizes the error function given in Eq. (4), this time summing over the short-sighted wavenumbers (step 10 below). These short-sighted wavenumbers are where the transmittance is low, and thus generally represent wavenumbers that were excluded in calculating the error function previously. The steps of the CO_2 slicing/sorting method used in this work are summarized as follows:

1. Choose model heights (layer boundaries) for the model atmosphere. Calculate R_{clr}. Calculate R_c, B_c, and t_c for each model height for the clear-sky atmosphere based on best estimates of temperature, water vapor, and trace gas amounts.
2. Calculate the LHS of Eq. (10).
3. Calculate the RHS of Eq. (10) for each model height and for each wavenumber.
4. Use CO_2 sorting to choose the best set of wavenumbers for the retrieval; these are typically between 720 and 755 cm^{-1}.
5. Find the height(s) at which the LHS and RHS agree best (interpolate to find where they cross or, if they never cross, determine where the difference is a minimum) for each wavenumber selected by CO_2 sorting.

Atmos. Meas. Tech. Discuss., doi:10.5194/amt-2016-49, 2016
Manuscript under review for journal Atmos. Meas. Tech.
Published: 7 March 2016

Atmospheric Measurement Techniques Discussions

6. Calculate the emissivity at the reference wavenumber, $\epsilon_c(\nu_0)$, using Eq. (6), for each cloud height (c) retrieved. This yields sets of cloud heights retrieved, comprised of one height for each selected wavenumber within each set, with corresponding reference emissivities. For example, there might be a set of cloud heights retrieved ($c_{\text{lower set}}(\nu)$) corresponding to heights below the inversion and a set ($c_{\text{higher set}}(\nu)$) above the inversion.

7. Calculate the error function as in Eq. (11) for the height retrieved at the first wavenumber, $c = c_{\text{lower set}}(\nu = \nu_1)$, using the corresponding $\epsilon_c(\nu_0)$ and $B_c(\nu)$, $t_c(\nu)$, and $R_c(\nu)$.

8. Repeat step 7 for each of the remaining selected wavenumbers ($\nu = \nu_2$, etc). Find $z_{c,\text{lower set}}$ that corresponds to the minimum error. This yields a single cloud height retrieval ($c_{\text{ret, lower set}}$).

9. Repeat 7 and 8 for the higher set of retrieved heights, yielding a single cloud height retrieval ($c_{\text{ret, higher set}}$).

10. To choose between $c_{\text{ret, lower set}}$ and $c_{\text{ret, higher set}}$, calculate the error function again for each of them. However, this time use the short-sighted wavenumbers; these are typically between 705 to 715 cm^{-1}.

4 Results

In this section we use the simulated spectra to compare the results of the MLEV and CO_2 slicing/sorting methods as adapted for this work against the "true" cloud base heights specified in the simulations. To understand how different hypothetical instrument specifications and varying amounts of ancillary information affect the results, the comparisons are made with and without imposed errors (e.g., instrument noise and uncertainty in the water vapor profile) and as functions of instrument resolution.

4.1 Cloud mask and retrieval capability

An important basic aspect of a cloud height retrieval algorithm is that it must be able to determine if there is a cloud present. Figure 2a shows a scatter plot of cloud height retrieved using CO_2 slicing/sorting vs. simulated cloud base-height. For these retrievals, no errors were imposed, so the only error present is model error. The spectral resolution is 0.5 cm^{-1}. The points are color-coded according to the cloud optical depth (in a real experiment, the optical depth will not be known). Cases with high PWV(> 2.9 cm) are indicated in red boxes; these points will be discussed later. The true cloud bases are offset by a small random factor so that the points are spread out slightly for better visibility; the discrete cloud base heights are evident for bases between 2 and 7 km.

Retrieved cloud base heights for clouds with very low optical depths (less than 0.5; red and orange points) stand out as having larger retrieval errors. These points constitute clouds that are below the radiance detection threshold and therefore need to be removed from the analysis. The cloud mask is set according to a threshold for a difference between measured and simulated radiance; for the wavenumbers selected using CO_2 sorting, a requirement that the root mean square (rms) difference between observed and clear-sky radiances differ by at least 2.2 RU is found to remove most low-accuracy points, as shown in Fig. 2b.

Atmos. Meas. Tech. Discuss., doi:10.5194/amt-2016-49, 2016
Manuscript under review for journal Atmos. Meas. Tech.
Published: 7 March 2016

Atmospheric Measurement Techniques Discussions

All cases with cloud optical depths below 0.25 were removed and many of the clouds with optical depths below 0.5 were removed.

Examining Fig. 2b, we see that retrieved cloud base is biased low for clouds above about 2 km (the mean bias is -0.93 km). The bias gets worse, roughly, as clouds get thinner. This bias occurs in large part because the emissivity is assumed to be constant with wavenumber, but actually varies slightly. For thinner clouds, the emissivity is typically larger at wavenumbers in the numerator of Eq. (9) than at the reference wavenumber (~ 811 cm^{-1}), in the denominator. Thus rather than cancelling out, the factor $\epsilon(\nu)/\epsilon(\nu_0)$ is typically about 1.05 for high, thin clouds, causing a bias of about -0.9 km on average. To remove this bias, Eq. (10) in step 3 is replaced with

$$\frac{R_{\rm obs}(\nu) - R_{\rm clr}(\nu)}{R_{\rm obs}(\nu_0) - R_{\rm clr}(\nu_0)} = \epsilon_{c,\rm rat}(\nu) \frac{B_c(\nu)t_c(\nu) + R_c(\nu) - R_{\rm clr}(\nu)}{B_c(\nu_0)t_c(\nu_0) + R_c(\nu_0) - R_{\rm clr}(\nu_0)}, \tag{12}$$

where $\epsilon_{c,\rm rat}(\nu)$ is determined at each trial cloud height (c) as an estimate of the ratio of the emissivity at ν to the emissivity at ν_0. For each trial height $\epsilon_{c,\rm rat}(\nu)$ is determined by first calculating the emissivity, $\epsilon_c(\nu)$, according to Eq. (6). While $\epsilon_c(\nu)$ should be smooth, the observed value is highly variable due to errors. Errors are expected to be lowest where the signal is strongest. Thus the next step is to select the wavenumbers where the signal is the strongest; for this a subset of the wavenumbers selected by CO_2 sorting is used. If fewer than 16 wavenumbers were selected by CO_2 sorting, then no emissivity smoothing is attempted; $\epsilon_{c,\rm rat}(\nu)$ is set to one; that is, Eq. (12) is abandoned in favor of Eq. (10). If at least 16 wavenumbers are selected by CO_2 sorting, then the points with the highest signal are used (for a resolution of 0.1 cm^{-1}, the ideal number appears to be about 90 to cover a sufficient portion of the spectral range, while for 0.5 cm^{-1} and up 30 points are sufficient). A straight line is fitted to the emissivity at the selected wavenumbers, and its value is divided by $\epsilon_c(\nu_0)$ to get an equation for $\epsilon_{c,\rm rat}$ for the selected wavenumbers. This equation is used for all wavenumbers within the range of the first and last of the selected wavenumbers. However, outside this range, $\epsilon_{c,\rm rat}$ is set to 1 because the weakness of the signal prohibits obtaining an estimate of the emissivity that is better than the assumption $\epsilon_c(\nu) = \epsilon_c(\nu_0)$, and examination of the true emissivity indicates that it may not continue to fall on the straight line determined by the fit at the selected wavenumbers.

Using a smooth, rather than constant, emissivity removes much of the low bias observed in Fig. 2b for clouds with bases above 2 km, as shown in Fig. 2c.

Returning to cases with high PWV (red boxes in panel a), note that these occur for cloud base heights near 2 and 4 km. We see in panels c and d that these clouds are retrieved quite accurately. It is generally true that these higher-PWV cases can be retrieved accurately even when errors are imposed, except for when large errors exist in PWV itself.

4.2 Comparison of CO_2 slicing/sorting and MLEV

Fig. 2d shows the scatter plot for cloud heights retrieved using MLEV. Comparing Figs. 2c and d, we see that both CO_2 slicing/sorting and MLEV are quite accurate for single-layer clouds in the absence of imposed errors. Fig. 3 shows histograms of error in retrieved cloud height, again for simulations with no imposed error and at a spectral resolution of 0.5 cm^{-1}. Note that the histograms are plotted with height on the vertical axis. For these and subsequent figures, we refer to low clouds as clouds with bases below 2 km. Medium to high clouds (bases from 2 to 8 km) are referred to as high clouds for brevity. As

Atmos. Meas. Tech. Discuss., doi:10.5194/amt-2016-49, 2016
Manuscript under review for journal Atmos. Meas. Tech.
Published: 7 March 2016

Atmospheric Measurement Techniques Discussions

shown in panels a and c, CO_2 slicing/sorting has a lower standard deviation for low clouds, while MLEV is slightly more accurate for high clouds (panels b and d).

In a real experiment, there are errors in the observed radiance (noise or bias) and in knowledge of the atmospheric state, most notably the temperature and humidity profiles. To probe the effects of these sources of error, cloud heights are retrieved with these errors imposed on the simulation of "observed" radiance (noise or bias) or on the temperature or water vapor profiles used in the retrieval.

Figures 4 and 5 are similar to Fig. 3 but include imposed error. For Fig. 4 a bias of 0.2 K is imposed in the temperature profile used in the retrievals at all heights, while for Fig. 5, a bias of -10% at all heights is imposed in the water vapor profile used in the retrieval. Positive biases in temperature or water vapor generally induce positive biases in simulated radiances and thus are accounted for by negative biases in cloud emission. Since temperature generally decreases with increasing height, this generally corresponds to a high bias in retrieved cloud heights. The reverse is generally true for negative biases in temperature and water vapor. For low clouds (cloud bases < 2 km) retrieved using CO_2 slicing/sorting, the negative bias in water vapor partially offsets the observed positive bias that is found in cases with no imposed error.

As Figs. 4 and 5 show, these errors affect high clouds much more than low clouds, for which retrievals remain quite accurate. This is not surprising given that high clouds generally have a weaker signal due to the larger atmospheric column below, and the greater sensitivity to the atmospheric column means they are more strongly affected by errors in knowledge of the atmospheric state.

Figures 4 and 5 also suggest that CO_2 slicing/sorting is more strongly affected by errors in the temperature profile used in the retrieval while MLEV is more strongly affected by errors in the water vapor profile. Detailed studies (Fig. 6) of a variety of errors reveal that MLEV is more accurate in the presence of biases in the observed radiance, and biases in temperature, while CO_2 slicing/sorting is more accurate in the presence of noise in the observed radiance and biases in water vapor. The panels of Fig. 6 are scatter plots similar to Fig. 2, but both CO_2 slicing/sorting (blue pluses) and MLEV (red dots) are plotted in each panel. Error sources and amounts are given in the titles (the black dashed line is discussed in Sect. 5.2). Note that the effect of a positive bias in observed cloudy-sky radiance is similar to that of a negative bias in simulated clear-sky radiance, and thus similar to the effects of negative biases in temperature and humidity.

Factors that complicate how errors affect retrievals using CO_2 slicing/sorting include errors in the fitting of the emissivity to a smooth function and changes in the strength of the apparent cloud signal, which can affect screening-out due to low signal. For example, positive biases can make the cloud signal look stronger (fewer cases screened out), while negative biases can make it look weaker, even resulting in negative radiances (more cases screened out). For MLEV, the consequences of errors are not as clear as for CO_2 slicing/sorting; indeed, both positive and negative biases in the water vapor profile (expressed as PWV in the figure) result in negative biases in retrieved cloud height.

4.3 Dependence of cloud height retrievals on resolution

Figure 7 shows the magnitude of the mean biases (solid lines) and the standard deviations (dashed lines) of errors in the retrieved cloud heights for MLEV (blue) and CO_2 slicing/sorting (red) as functions of instrument resolution. Upper panels are

Atmos. Meas. Tech. Discuss., doi:10.5194/amt-2016-49, 2016
Manuscript under review for journal Atmos. Meas. Tech.
Published: 7 March 2016

Atmospheric Measurement Techniques Discussions

for low clouds and lower panels are for high clouds. The left panels show means and biases in the absence of imposed error, and the right panels are for cases that include imposed errors (0.1 RU noise and a temperature bias of -0.1 K). Note that mean biases are positive for low clouds and negative for high clouds; the figure shows the absolute values of the biases.

For all cases, retrieval errors increase overall as resolution becomes coarser, from 0.1 to 8 cm^{-1}. While MLEV and CO_2 slicing/sorting give similar results at a resolution of 0.1 cm^{-1}, errors generally grow larger for MLEV with coarsening resolution than for CO_2 slicing/sorting. For low clouds the standard deviations diverge immediately, at 0.5 or 1 cm^{-1}, while mean biases diverge at 2 cm^{-1}. For high clouds variability is more complicated: in the absence of imposed errors neither MLEV nor CO_2 slicing/sorting are clearly better than the other, while when the imposed errors are present, retrieval errors grow larger with coarsening resolution for MLEV.

5 Discussion

5.1 Context with past studies

Mahesh et al. (2001a) assume a variation of 3% in the ratio of emissivities $\epsilon(\nu)/\epsilon(\nu_0)$ (i.e. error due to the assumption that emissivity is constant with wavenumber over the spectral region used). In their analysis, this source of uncertainty leads to uncertainty in retrieved cloud-base pressure of 5 to 13 mb (for a zenith angle of 45 degrees). Converting these to errors in cloud-base height gives error estimates of 0.03 to 0.11 km for low clouds (bases of 0.1 to 1 km) and 0.14 km for a single high cloud at 2.1 km. In this work, we find that for high, thin clouds the variation in $\epsilon(\nu)/\epsilon(\nu_0)$ is closer to 5%, resulting in biases of about -0.9 km for high clouds (above $\sim$2 km, for a zenith view). Furthermore, we estimate that errors in retrieved height due to other sources of model error are $\sim 0.21 \pm 0.35$ km for low clouds and -0.19 $\pm$ 0.41 km for high clouds. Thus this work expands on the error analysis of Mahesh et al. (2001a) and indicates that retrieval errors for the CO_2 slicing model applied to downwelling radiances are larger than previously predicted. However, errors in actual cases will depend on the specific set of clouds sampled.

Figs. 3-5 were plotted to be comparable to Figs. 7, 8, 11 and 14 of Holz et al. (2006), which show similar histograms for CO_2 slicing/sorting, CO_2 slicing (without sorting; not included here as a separate category) and MLEV. Note, however, that Holz et al. (2006) compare cloud-top height retrieved from upwelling (aircraft-based) infrared radiances (nadir view, 0.5 cm^{-1} instrument resolution) to cloud heights from lidar measurements, whereas we compare cloud heights retrieved from simulated downwelling radiances at the surface to known model cloud-base heights. Thus our results are not suited for detailed comparisons. However, some general observations can be made.

The results of Holz et al. (2006) suggest that CO_2 slicing/sorting is more accurate than MLEV for retrievals of optically thin clouds ($\tau < 1.0$) from measurements of upwelling radiance. This study indicates that, for downwelling radiances, the two are roughly equivalent, and highly accurate, in the absence of errors, while in the presence of errors accuracy is highly dependent on the source of error. As an example, this work shows that humidity biases cause smaller errors for CO_2 slicing/sorting than for MLEV; thus one explanation for the higher accuracy Holz et al. found for CO_2 slicing/sorting could be errors in the humidity profiles they used. Finally, Holz et al. state that retrievals are challenging for clouds below 3 km using upwelling

Atmos. Meas. Tech. Discuss., doi:10.5194/amt-2016-49, 2016
Manuscript under review for journal Atmos. Meas. Tech.
Published: 7 March 2016

Atmospheric Measurement Techniques Discussions

radiances. Since low clouds are retrieved most accurately using downwelling radiances, retrievals from surface-based infrared spectrometers provide an important complementarity.

5.2 Combining MLEV and CO_2 slicing/sorting

The fact that MLEV and CO_2 slicing/sorting show different susceptibilities to different sources of errors suggests that the best method is to use them in combination. This is reasonable as they use overlapping, but distinct frequency regions. The exact details of how this is done will depend on the relative magnitudes of errors for a given case, which in turn depends on knowledge of the atmospheric state. But a few details are worth pointing out here.

Both MLEV and CO_2 slicing/sorting are fairly accurate for low clouds, even in the presence of errors, with the exception of large biases in the water vapor profile for MLEV. However, this knowledge is not useful if low clouds cannot be distinguished from high clouds. High clouds can be identified in several ways. Referring back to Fig. 6, note the dashed line in each panel. For all errors shown, only a few points fall in the region to the upper left of this line. This indicates that large positive biases are generally not found for retrievals of low clouds. Instead, positive biases are generally limited to the value shown by the line. For example, clouds at 1 km are not retrieved above 3 km. This means that if a high height is retrieved, the true cloud-base is probably high. Furthermore, cloud heights retrieved for low clouds tend to agree fairly well for MLEV and CO_2 slicing, while retrieved cloud heights for high clouds often disagree. Thus if MLEV and CO_2 slicing/sorting disagree, the true cloud-base is probably high. This allows accurate categorization of most clouds into low or high; there are few cases where the retrieved heights are biased low by 2 km or more for both CO_2 slicing/sorting and MLEV.

Methods for combining MLEV and CO_2 slicing/sorting are worth pursuing but are beyond the scope of this work. They could include combining them at the algorithmic level: for example, in a Bayesian analysis that determines the optimal solution based on the intersection of the mean $\pm$ 1 standard deviation probabilities for CO_2 slicing/sorting and MLEV. Or they could be combined post-retrieval by calculating a weighted combination of retrieved cloud heights for the two methods, where the weights depend on the uncertainty levels of the radiance, knowledge of the atmospheric state, and retrieved heights. Regardless, how best to combine CO_2 slicing/sorting and MLEV will depend on resolution and the magnitudes of sources of error and will require estimates of how errors are propagated into errors in retrieved cloud heights. The extra computational time taken for running both CO_2 slicing/sorting and MLEV is minimal because the most time-consuming computations are the calculations of B_c, t_c and R_c for each model layer, and this set of calculations is identical for the two methods (see step 1 for each method in Sect. 3.2 and Sect. 3.3).

5.3 Effect of resolution on retrieval

For CO_2 slicing/sorting in the absence of errors, the mean bias in retrievals for high clouds increases rapidly with resolution from $\sim$ 0 km at 2 cm^{-1} to -1 km at 4 cm^{-1} (refer back to dashed red line in Fig. 7b, but note that the figures shows the absolute value of the mean bias). This is primarily due to the assumption that the emissivity is constant. As described previously, the variation of the emissivity with wavenumber results in a mean bias of -0.93 at a resolution of 0.5 cm^{-1}, but this bias is removed to a large extent by fitting the emissivity at high-signal points to a best-fit line and using the best-fit line to calculate a

Atmos. Meas. Tech. Discuss., doi:10.5194/amt-2016-49, 2016
Manuscript under review for journal Atmos. Meas. Tech.
Published: 7 March 2016

Atmospheric Measurement Techniques Discussions

smoothly varying (linear rather than constant) emissivity. At resolutions coarser than ~ 2 cm^{-1}, this correction is hindered by an insufficient number of points, and the bias reappears; note that a bias of -0.93 explains much of the magnitude of the bias shown for CO_2 slicing/sorting in Fig. 7b at 4 and 8 cm^{-1}. A similar increase is evident when errors are imposed (dashed red line in Fig. 7d), but it occurs at a lower resolution (1 to 2 cm^{-1}) and is superimposed on a large negative bias ($\sim$1.2 km) due to the imposed errors.

Because different sources of error affect the CO_2 slicing/sorting and MLEV retrievals differently, errors in creating Fig. 7 were chosen so that retrieval errors roughly agree at a resolution of 0.1 cm^{-1} (Fig. 7 c and d) so that the variation with coarsening resolution could be examined in a comparable manner. Comparing cases with and without the imposed error, for low clouds, mean biases are actually reduced when the error is imposed (compare Figs. 7a and c). This occurs because the negative bias imposed on the temperature profile biases the retrieved cloud heights low; the negative bias in retrieved cloud height partially counteracts the positive bias that occurs due to model assumptions. The opposite is true for high clouds: negative biases from the temperature profile errors exacerbate low-biases due to model assumptions (recall that absolute biases are plotted; actual biases are positive for low clouds and negative for high clouds). Thus for the example shown in the figure, retrieval errors are worsened by the imposed errors for high clouds. If a positive bias in temperature were imposed, the bias would increase positive biases for low clouds and decrease negative biases for high clouds. If both positive and negative temperature biases were imposed, retrieval biases would be unchanged.

While imposed errors may sometimes counteract mean biases, they nevertheless increase the spread of errors (indicating that errors for individual cases are overall higher) as shown by the increases in standard deviation when errors are imposed (solid lines in right-hand panels of Fig. 7 are generally higher than in left-hand panels). However, note that there is less dependence on resolution in the presence of errors (solid lines in right panels of Fig. 7 are flatter than in left panels). Thus in the presence of errors, there is less benefit to finer resolution. For CO_2 slicing/sorting, finer resolution has little advantage except that it allows the removal of the model-induced low bias in retrieved cloud height due to assuming the emissivity is constant, as described previously. However, if errors were larger, this advantage would likely disappear as well.

The errors imposed on the retrievals in the right panels are moderate: the noise is only 0.1 RU and the bias in temperature profiles is only -0.1 K, yet the increase in retrieval errors is fairly large; for CO_2 slicing/sorting retrieval errors roughly double. However, a few points are worth noting. First, bias errors represent a worst-case scenario; errors that vary in sign with height will have a smaller effect. Second, the magnitude of the errors that are allowed depends directly on the threshold used for cloud detection. Here a threshold of 2.2 RU was used, allowing clouds with optical depths as low as 0.25-0.5 to be retrieved. A stricter threshold would result in greater retrieval accuracy, at a cost of eliminating more thin clouds. In other words, retrieval accuracy is directly dependent on cloud signal, and will be greater for thicker clouds. This is demonstrated in Fig. 8, where the x-axis in panels b and c is cloud signal, computed as the root-mean-square difference between cloudy and clear-sky radiance at the wavenumbers used in the retrieval. For this case (resolution of 4 cm^{-1}, with imposed noise and temperature bias), the absolute cloud height error decreases from a maximum of 3.1 km for the lowest cloud signal, to 0.2 km for the highest signal (panel c). Cloud-height retrieval accuracy also decreases with cloud height; panel a shows that the absolute value of the error increases

Atmos. Meas. Tech. Discuss., doi:10.5194/amt-2016-49, 2016
Manuscript under review for journal Atmos. Meas. Tech.
Published: 7 March 2016

Atmospheric Measurement Techniques Discussions

with cloud height. This is partly because higher clouds tend to have lower signal, but also occurs independent of cloud signal. For example, for a cloud signal of ∼3 RU retrieval errors vary from 0 to 3.5 km (colors in panel a).

5.4 Error and instrument characteristics

For cloud retrievals in the polar regions using an autonomous infrared spectrometer, noise and radiation bias represent instrument characteristics, while errors in the atmospheric profiles will depend on the accuracy of knowledge of the atmospheric state. In remote locations, this will in turn depend on the accuracy of reanalysis data, such as from the European Centre for Medium-Range Forecasting (ECMWF) Interim reanalysis dataset (ERA-Interim; Dee et al., 2011).

Wesslen et al. (2014) measured temperature and humidity profiles and compared them to ERA-Interim. These profiles were not assimilated into the reanalyses, and the location of the measurements was distant from radiosonde assimilation sources; thus, we assume their estimated errors in temperature profiles are similar to what an autonomous spectrometer would experience in remote locations, except that the temperature at the surface will be measured and thus known very accurately. Thus we assume errors of 0 K at the surface increasing to 0.5 K at 0.1 km. For water vapor, they find mean errors to be typically positive and below 2% for the first 3 km, after which they increase to 5 to 10% from 4 to 8 km. For this work we assume a relative bias of 3% throughout the atmosphere. Again, we assume the relative humidity will be measured to high accuracy at the surface and correct the surface error to 0%. This represents an underestimate of error in the upper atmosphere; however, most of the water vapor is in the lower atmosphere, where this represents an overestimate of error. CO_2 errors are expected to be on the order of 0.5%, based on the work of Alkhaled et al. (2008). This source of error is expected to be quite small.

Fig. 7 (shown previously) can be used as a guide to choose the ideal instrument resolution for an autonomous infrared spectrometer. (It is important to note that Fig. 7c and d are based on only one set of imposed errors (0.1 RU noise and 0.1 K temperature bias), and thus results may be different for different imposed errors.) In the presence of these errors, retrieval accuracy is roughly equivalent at 0.1 and 0.5 cm^{-1}. For MLEV, large increases begin at about 1 cm^{-1}. For CO_2 slicing/sorting, in contrast, errors remain flat up to resolutions as coarse as 4 cm^{-1}, except for biases in high clouds, which are about 50% higher at 4 cm^{-1}. This suggests that a resolution of 2 cm^{-1} is adequate for CO_2 slicing/sorting. The decision of the exact resolution to use will depend on the capability of achieving the desired noise level, since throughput, and thus the signal-to-noise, increase as resolution becomes coarser.

Table 1 shows error estimates calculated for a resolution of 0.5 cm^{-1} for a variety of sources of error, for low clouds. Table 2 is the same, but for high clouds. After screening out cases with low cloud signal (see the columns indicated with Omit.), errors in retrieved cloud height (retrieved - true cloud-base height) are calculated for each remaining case. The mean error, representing the mean bias in retrieved cloud heights, and the standard deviation are given in the table. The effect of model error, which is present even when no errors are imposed, is shown in the top row. Because model error is present for all retrievals, the value in the table for each source of error is an overestimate. To determine the error in retrieved height due to a given source of error, the effect of model error needs to be removed. For mean biases, it can simply be subtracted out, while for standard deviations it should be removed in quadrature. As shown in the table, the effect of the varying temperature error based on Wesslen et al. (2014) was found to be roughly equivalent to the effect of a positive temperature bias of 0.2 K. For water

Atmos. Meas. Tech. Discuss., doi:10.5194/amt-2016-49, 2016
Manuscript under review for journal Atmos. Meas. Tech.
Published: 7 March 2016

Atmospheric Measurement Techniques Discussions

vapor, biases of $\pm$ 3% at all heights were assumed to be roughly equivalent to the errors found by Wesslen et al. (2014) for ERA-Interim. For comparison, water vapor errors of 10% were also calculated. CO_2 errors of $\pm$ 0.5% were found to produce negligible errors; that is, errors were approximately the same as for model error only. As the table shows, for low clouds, mean biases are almost always positive and are $\leq$ 0.74 km for all sources of error tested, illustrating the accuracy with which low clouds can be retrieved. For high clouds, the situation is quite different; standard deviations can be 2 km or more for a single source of error.

The table also gives the number of cases omitted for each source of error. Cases were omitted if the root-mean-square radiance difference for cloudy - clear sky conditions ($R_{\text{obs}} - R_{\text{clr}}$) was greater than a chosen threshold (2.2 RU). The threshold was chosen that eliminated all clouds with optical depths less than 0.25 and most with optical depths less than 0.5 in the absence of imposed error (referring back to Fig. 2 a and b). This typically eliminated less than about 20 low-cloud cases. For high clouds, about half (24-36 out of 67) of the clouds were screened out. High clouds emit less because they are colder and typically thinner than low clouds; furthermore they have a longer transmission path length through the atmosphere. Thus it seems likely that applying such a threshold to real measurements will also screen out a greater proportion of high clouds (this was true in our dataset despite the fact there is no statistical difference between the optical depths of high and low clouds). More clouds are screened out for errors that reduce the cloudy-sky radiance or increase the clear-sky radiance. Tuning the threshold to a higher value will remove more low-signal cases, particularly high clouds.

The final row of each table gives an estimate of combined sources of error. This included noise (0.1 RU), radiation bias (0.1 RU), temperature biases of $\pm$ 0.2 K, and water vapor biases of $\pm$ 3%. To calculate the combined errors, first the effect of model error was removed from all error estimates save one (so that model error wouldn't be included multiple times) for both mean biases in retrievals and standard deviations. Next, errors for positive and negative biases were averaged. Finally, retrieval biases were summed and standard deviations were added in quadrature. For these error levels, for high clouds and a resolution of 0.5 cm^{-1}, mean biases are better than $\sim$2.5 km and standard deviations are less than 2 km.

If these instrument characteristics are difficult to achieve, it is also possible to screen out more thin cloud cases by increasing the cloud-signal threshold. The threshold of 2.2 RU removed almost half of the clouds with bases of 2 km and above; a larger threshold would exclude even more. Higher instrumental errors are tolerable for low clouds; for example noise of 0.8 RU and bias of 0.4 RU errors correspond to errors of $\sim$0.3 $\pm$ km for low clouds. Furthermore, as discussed previously, accuracy can be improved and most high clouds erroneously identified as low can be correctly identified by combining the CO_2 slicing/sorting and MLEV methods.

The statistics of cloud base heights used in this work are similar to those measured in the Arctic (see Cox et al., 2016, and references therein), with 79% of the clouds below 2 km. Low clouds are also common in the Antarctic (Bromwich et al., 2012; Mahesh et al., 2005). Thus a surface-based spectrometer would be of the greatest benefit for retrieving the heights of low clouds, which are common in the polar regions.

Atmos. Meas. Tech. Discuss., doi:10.5194/amt-2016-49, 2016
Manuscript under review for journal Atmos. Meas. Tech.
Published: 7 March 2016

Atmospheric Measurement Techniques Discussions

6 Conclusions

Two established methods for retrieving cloud height from upwelling infrared radiances are modified for retrievals from downwelling infrared radiances: the Minimum Local Emissivity Variance (MLEV) and the CO_2 slicing/sorting method. Modifications to CO_2 slicing/sorting make use of the method of Mahesh et al. (2001a) for CO_2 slicing of downwelling radiances. For CO_2 slicing/sorting, it was determined that a low bias (approximately -0.9 km) is present in retrievals of clouds with bases of 2 km or higher; a correction to this bias is presented that assumes a smooth, rather than constant emissivity at wavenumbers selected by CO_2 sorting ($\sim$720 to 811 cm^{-1}). However, it is found that this correction can only be applied when other errors are low.

Working towards the goal of assessing the feasibility of cloud height retrievals from an infrared spectrometer designed to be used in remote polar locations, and the instrumental considerations (noise and bias in measured radiances) permitting useful retrievals, errors in cloud-height retrievals using the two methods are assessed for simulated radiance observations. Simulated radiances include single-layer, mixed-phase clouds for a variety cloud and atmospheric conditions characteristic of the Arctic, at resolutions of 0.1 to 8 cm^{-1}. Retrieval errors are estimated for instrumental sources of error and errors in the atmospheric state that are likely to be experienced in measurements.

In the absence of imposed errors, cloud height retrievals from simulated spectra using CO_2 slicing/sorting and MLEV are found to have roughly equivalent, high accuracies at resolutions of 0.5 cm^{-1} or finer. For example, at 0.5 cm^{-1}, mean biases are found to be $\sim$ 0.2 km for low clouds (bases below 2 km, $\sim$143 cases) and -0.2 km for high clouds (bases $\geq$ 2 km, 39 cases). As resolution becomes coarser, errors increase. For low clouds, CO_2 slicing/sorting is found to be more accurate than MLEV at resolutions coarser than 0.5 cm^{-1}. For high clouds, the situation is more complicated: CO_2 slicing/sorting is more accurate from about 1 to 2.5 cm^{-1}, and MLEV is more accurate from 2.5 to 8 cm^{-1}. However, in the presence of errors, the dependence on resolution is weakened. Furthermore, the two methods are found to have differing sensitivities to different sources of error: CO_2 slicing/sorting is more sensitive to bias in observed radiation and errors in the temperature profile, while MLEV is more sensitive to noise and humidity errors. This complementarity suggests that an approach that combines the two methods is ideal. In particular (for expected error magnitudes), it can be assumed that the cloud base is high if either method retrieves a high cloud, or if the two methods disagree widely. This can be extremely helpful to improve or screen out cases where one method fails completely, e.g. when a near-surface height is retrieved for a cloud base above 2 km for only one method.

Retrieval accuracy is found to decrease with cloud signal, where cloud signal is defined to be the rms difference, at the selected wavenumbers, between observed and clear-sky radiances. A cloud-signal threshold of 2.2 RU is found to screen out all cases used here with clouds having optical depths below 0.25 and many clouds with optical depths below 0.5. Proportionally more high clouds are screened out than low clouds because high clouds typically have lower signal (because they emit less, due to lower cloud temperature, and less cloud emission reaches the surface). However, retrievals for high clouds are also found to be less accurate independent of cloud signal. Indeed, errors have a small effect on retrievals of low clouds but a large effect on high clouds. For real clouds, high clouds are also typically thinner optically than low clouds, thus applying the threshold to real observations is expected to remove even more high-cloud cases, proportionally to low-cloud cases.

Atmos. Meas. Tech. Discuss., doi:10.5194/amt-2016-49, 2016
Manuscript under review for journal Atmos. Meas. Tech.
Published: 7 March 2016

Expected errors in the atmospheric state indicate that a resolution of 0.5 cm^{-1}, instrument noise level of 0.1 RU and bias of 0.1 RU would permit retrievals of high clouds to an accuracy of -2 $\pm$ 2 km for both methods. Accuracy for low clouds would be $\sim 0.2 \pm 0.5$ km. If these instrument characteristics are not feasible, retrievals may be performed for a smaller subset of thicker clouds by increasing the cloud-signal threshold, which would exclude a large portion of high clouds. Furthermore, higher instrumental errors are tolerable for low clouds; for example noise of 0.8 RU and bias of 0.4 RU errors correspond to errors of about $\sim 0.3 \pm$ km for low clouds. For a fixed noise level, the ideal instrument resolution is 0.5 cm^{-1} for MLEV and 0.5 to 2 cm^{-1} for CO_2 slicing/sorting. However, there are likely trade-offs between noise and instrument resolution. The detailed analysis presented here can help optimize instrument characteristics.

The sensitivity demonstrated here for a surface-based infrared spectrometer to low clouds, which are most common in polar regions, is an important complement to satellite-based measurements, particularly infrared instruments, for which low-level cloud retrievals are challenging.

7 Data Availability

The dataset of perfect resolution downwelling radiance spectra characteristic of the Arctic (Cox et al., 2015) is available on the Arctic Observing Network (AON) Arctic data repository (at https://www.aoncadis.org/dataset/AAIRO_spectra.html; doi:10.5065/D61J97TT) and is described by Cox et al. (2016). Computer codes for creating cloudy spectra (runDisort_mat and runDisort_py), which use DISORT (Stamnes et al., 1988), are available at https://github.com/prowe12; see also Rowe et al. (2013).

Acknowledgements. The authors acknowledge funding from National Science Foundation grant, ARC-1108451. C.J.C. acknowledges funding from the Arctic Research Program of the NOAA Climate Program Office and the Cooperative Institute for Research in Environmental Sciences (CIRES) Visiting Fellowship Program. P.M.R. acknowledges funding from Consejo Nacional de Ciencia y Tecnología (CONICYT)-Anillos, Preis ACT1410 and from the National Science Foundation under PLR 1543236. Any opinions, findings, and conclusions or recommendations expressed in this material are those of the authors and do not necessarily reflect the views of the National Science Foundation. The authors are also grateful for useful conversations with S. Neshyba (U. Puget Sound).

Atmos. Meas. Tech. Discuss., doi:10.5194/amt-2016-49, 2016
Manuscript under review for journal Atmos. Meas. Tech.
Published: 7 March 2016

References

Alkhaled, A. A., Michalak, A. M., Kawa, S. R., Olsen, S. C., and Wang, J.-W.: A global evaluation of the regional spatial variability of column integrated CO_2 distributions, J. Geophys. Res., 113, D20,303–17, doi:10.1029/2007JD009693, 2008.

Bromwich, D. H., Nicolas, J. P., Hines, K. M., Kay, J. E., Key, E. L., Lazzara, M. A., Lubin, D., McFarquhar, G. M., Gorodetskaya, I. V., Grosvenor, D. P., Lachlan-Cope, T., and van Lipzig, N. P.: Tropospheric clouds in Antarctica, Rev. Geophys., 50, RG1004, doi:10.1029/2011RG000363, 2012.

Cesana, G. and Chepfer, H.: Evaluation of the cloud thermodynamic phase in a climate model using CALIPSO-GOCCP, J. Geophys. Res. Atmos., 118, 7922–7937, doi:10.1002/jgrd.50376, 2013.

Cesana, G., Kay, J. E., Chepfer, H., English, J. M., and de Boer, G.: Ubiquitous low-level liquid-containing Arctic clouds: New observations and climate model constraints from CALIPSO-GOCCP, Geophys. Res. Lett., 39, L20 804, doi:10.1029/2012GL053385, 2012.

Choi, Y.-S., Kim, B. M., Hur, S. K., Kim, S. J., Kim, J. H., and Ho, C.-H.: Connecting early summer cloud-controlled sunlight and late summer sea ice in the Arctic, J. Geophys. Res. Atmos., 119, 11,087–11,099, doi:10.1002/2014JD022013, 2014.

Christensen, P. R., Jakosky, B. M., Mehall, G. L., Kieffer, H. H., Ferry, S., Malin, M. C., McSween Jr, H. Y., Nealson, K., Silverman, S. H., Ferry, S., Caplinger, M., and Ravine, M.: The Thermal Emission Imaging System (THEMIS) for the Mars 2001 Odyssey Mission, Space Science Reviews, 110, 85–130, doi:10.1023/B:SPAC.0000021008.16305.94, 2004.

Clough, S., Iacono, M. J., and Moncet, J. L.: Line-by-line calculations of atmospheric fluxes and cooling rates: Application to water vapor, J. Geophys. Res. Atmos., 97, 15 761–15 785, 1992.

Clough, S., Shephard, M. W., Shephard, M. W., Mlawer, E. J., Delamere, J. S., Iacono, M. J., Cady-Pereira, K., Boukabara, S., and Brown, P. D.: Atmospheric radiative transfer modeling: a summary of the AER codes, Journal of Quantitative Spectroscopy and Radiative Transfer, 91, 233–244, doi:10.1016/j.jqsrt.2004.05.058, 2005.

Cox, C., Walden, V. P., and Rowe, P. M.: A comparison of the atmospheric conditions at Eureka, Canada, and Barrow, Alaska (2006-2008), J. Geophys. Res., 117, D12 204, doi:10.1029/2011JD017164, 2012.

Cox, C., Turner, D. D., Rowe, P. M., Shupe, M., and Walden, V. P.: Cloud Microphysical Properties Retrieved from Downwelling Infrared Radiance Measurements Made at Eureka, Nunavut, Canada (2006–09), J. Appl. Meteor. Climatol., 53, 772–791, doi:20.1175/JAMC-D-13-0113.1, 2014.

Cox, C., Rowe, P., and Walden, V. P.: Simulated Spectra for Autonomous Arctic Infrared Observer, UCAR/NCAR - CISL - ACADIS, dataset, doi:10.5065/D61J97TT, 2015.

Cox, C., Rowe, P. M., Neshyba, S., and Walden, V. P.: A synthetic data set of high-spectral resolution infrared spectra for the Arctic Atmosphere, Earth Syst. Sci. Data Discuss. (in review for Earth Syst. Sci. Data), doi:10.5194/essd-2015-40, 2016.

Dee, D. P., Uppala, S. M., Simmons, A. J., Berrisford, P., Poli, P., Kobayashi, S., Andrae, U., Balmaseda, M. A., Balsamo, G., Bauer, P., Bechtold, P., Beljaars, A. C. M., van de Berg, L., Bidlot, J., Bormann, N., Delsol, C., Dragani, R., Fuentes, M., Geer, A. J., Haimberger, L., Healy, S. B., Hersbach, H., Hólm, E. V., Isaksen, L., Kållberg, P., Köhler, M., Matricardi, M., McNally, A. P., Monge-Sanz, B. M., Morcrette, J. J., Park, B. K., Peubey, C., de Rosnay, P., Tavolato, C., Thépaut, J. N., and Vitart, F.: The ERA-Interim reanalysis: configuration and performance of the data assimilation system, Q.J.R. Meteorol. Soc., 137, 553–597, doi:10.1002/qj.828, 2011.

Francis, J. and Hunter, E.: Changes in the fabric of the Arctic's greenhouse blanket, Environ. Res. Lett., 2, 045 011, doi:10.1088/1748-9326/2/4/045011, 2007.

Hines, K. M., Bromwich, D. H., Rasch, P., and Iacono, M. J.: Antarctic Clouds and Radiation within the NCAR Climate Models, J. Climate, 17, 1198–1212, 2004.

Holz, R. E., Ackerman, S. A., Antonelli, P., Nagle, F., Knuteson, R. O., McGill, M., Hlavka, D. L., and Hart, W. D.: An Improvement to the High-Spectral-Resolution CO_2-Slicing Cloud-Top Altitude Retrieval, J. Atmos. Oceanic Technol., 23, 653–670, doi:10.1175/JTECH1877.1, 2006.

Huang, H.-L., Smith, W. L., Li, J., Antonelli, P., Wu, X., Knuteson, R. O., Huang, B., and Osborne, B. J.: Minimum local emissivity variance retrieval of cloud altitude and effective spectral emissivity-simulation and initial verification, J. Appl. Meteor., 43, 795–809, 2004.

Kahn, B. H., Eldering, A., Braverman, A. J., Fetzer, E. J., Jiang, J. H., Fishbein, E. F., and Wu, D. L.: Toward the characterization of upper tropospheric clouds using Atmospheric Infrared Sounder and Microwave Limb Sounder observations, J. Geophys. Res., 112, D05 202, doi:10.1029/2006JD007336, 2007.

Kay, J. E., L'Ecuyer, T., Gettelman, A., Stephens, G. L., and O'Dell, C.: The contribution of cloud and radiation anomalies to the 2007 Arctic sea ice extent minimum, Geophys. Res. Lett., 35, L08 503, doi:10.1029/2008GL033451, 2008.

Mahesh, A., Walden, V. P., and Warren, S. G.: Ground-based infrared remote sensing of cloud properties over the Antarctic Plateau. Part I: Cloud-base heights, J. Appl. Meteor., 40, 1265–1278, 2001a.

Mahesh, A., Walden, V. P., and Warren, S. G.: Ground-based infrared remote sensing of cloud properties over the Antarctic Plateau. Part II: Cloud optical depths and particle sizes, J. Appl. Meteor., 40, 1279–1294, 2001b.

Mahesh, A., Campbell, J. R., and Spinhirne, J. D.: Multi-year measurements of cloud base heights at South Pole by lidar, Geophys. Res. Lett., 32, L09 812, 2005.

Mariani, Z., Strong, K., Palm, M., Lindenmaier, R., Adams, C., Zhao, X., Savastiouk, V., McElroy, C. T., Goutail, F., and Drummond, J. R.: Year-round retrievals of trace gases in the Arctic using the Extended-range Atmospheric Emitted Radiance Interferometer, Atmos. Meas. Tech., 6, 1549–1565, doi:10.5194/amt-6-1549-2013, 2013.

Menzel, W. P., Smith, W. L., and Stewart, T. R.: Improved cloud motion wind vector and altitude assignment using VAS, J. Climate Appl. Meteor., 22, 377–384, doi:10.1175/1520-0450(1983)022<0377:ICMWVA>2.0.CO;2, 1983.

Minnis, P., Chakrapani, V., Doelling, D. R., Nguyen, L., Palikonda, R., Spangenberg, D. A., Uttal, T., Arduini, R. F., and Shupe, M.: Cloud coverage and height during FIRE ACE derived from AVHRR data, J. Geophys. Res., 106, 15 215–15 232, doi:10.1029/2000JD900437, 2001.

Neshyba, S. and Rathke, C.: Statistics of Arctic cloud downwelling infrared emissivity, J. Geophys. Res., 108, 4468, doi:10.1029/2002JD003157, 2003.

Pithan, F. and Mauritsen, T.: Arctic amplification dominated by temperature feedbacks in contemporary climate models, Nature Geosci, 7, 181–184, doi:10.1038/NGEO2071, 2014.

Pithan, F., Medeiros, B., and Mauritsen, T.: Mixed-phase clouds cause climate model biases in Arctic wintertime temperature inversions, Clim. Dyn., 43, 289–303, doi:10.1007/s00382-013-1964-9, 2014.

Rathke, C., Fischer, J., Neshyba, S., and Shupe, M.: Improving IR cloud phase determination with 20 microns spectral observations, Geophys. Res. Lett., 29, 50–1–50–4, doi:10.1029/2001GL014594, 2002.

Rowe, P. M., Miloshevich, L. M., Turner, D. D., and Walden, V. P.: Dry Bias in Vaisala RS90 Radiosonde Humidity Profiles over Antarctica, J. Atmos. Oceanic Technol., 25, 1529–1541, doi:10.1175/2008JTECHA1009.1, 2008.

Rowe, P. M., Neshyba, S., and Walden, V. P.: Radiative consequences of low-temperature infrared refractive indices for supercooled water clouds, Atmos. Chem. Phys., 13, 11 925–11 933, 2013.

Schweiger, A. J., Lindsay, R. W., Vavrus, S., and Francis, J.: Relationships between Arctic Sea Ice and Clouds during Autumn, J. Climate, 21, 4799–4810, doi:10.1175/2008JCLI2156.1, 2008a.

Schweiger, A. J., Zhang, J., Lindsay, R. W., and Steele, M.: Did unusually sunny skies help drive the record sea ice minimum of 2007?, Geophys. Res. Lett., 35, L10 503, doi:10.1029/2008GL033463, 2008b.

Shupe, M., Turner, D. D., Walden, V. P., Bennartz, R., Cadeddu, M. P., Castellani, B. B., Cox, C., Hudak, D. R., Kulie, M. S., Miller, N. B., Neely, R. R., Neff, W., and Rowe, P. M.: High and Dry: New Observations of Tropospheric and Cloud Properties above the Greenland Ice Sheet, Bulletin of the American Meteorological Society, 94, 169–186, doi:10.1175/BAMS-D-11-00249.1, 2013.

Smith, W. L. and Platt, C.: Comparison of satellite-deduced cloud heights with indications from radiosonde and ground-based laser measurements, J. Appl. Meteor., 17, 1796–1802, doi:10.1175/1520-0450(1978)017<1796:COSDCH>2.0.CO;2, 1978.

Stamnes, K., Tsay, S.-C., Tsay, S.-C., Wiscombe, W. J., and Jayaweera, K.: Numerically stable algorithm for discrete-ordinate-method radiative transfer in multiple scattering and emitting layered media, Appl. Opt., 27, 2502–2509, 1988.

Stamnes, K., Ellingson, R. G., Curry, J. A., Walsh, J. E., and Zak, B. D.: Review of science issues, deployment strategy, and status for the ARM North Slope of Alaska-Adjacent Arctic Ocean climate research site, J. Climate, 12, 46–63, doi:10.1175/1520-0442-12.1.46, 1999.

Town, M. S., Walden, V. P., and Warren, S. G.: Cloud cover over the South Pole from visual observations, satellite retrievals, and surface-based infrared radiation measurements, J. Climate, 20, 544–559, 2007.

Uttal, T., Curry, J. A., Mcphee, M. G., Perovich, D. K., Moritz, R. E., Maslanik, J. A., Guest, P. S., Stern, H. L., Moore, J. A., Turenne, R., Heiberg, A., Serreze, M. C., Wylie, D. P., Persson, O., Paulson, C. A., Halle, C., Morison, J. H., Wheeler, P. A., Makshtas, A., Welch, H., Shupe, M., Intrieri, J. M., Stamnes, K., Lindsey, R. W., Pinkel, R., Pegau, W. S., Stanton, T. P., and Grenfeld, T. C.: Surface heat budget of the Arctic Ocean, Bull. Amer. Meteor. Soc., 83, 255–275, doi:10.1175/1520-0477(2002)083<0255:SHBOTA>2.3.CO;2, 2002.

Verlinde, J., Harrington, J., McFarquhar, G. M., Yannuzzi, V. T., Avramov, A., Greenberg, S., Johnson, N., Zhang, G., Poellot, M. R., Mather, J. H., Turner, D. D., Eloranta, E. W., Zak, B. D., Prenni, A. J., Daniel, J. S., Kok, G. L., Tobin, D. C., Holz, R. E., Sassen, K., Spangenberg, D., Minnis, P., Tooman, T. P., Ivey, M. D., Richardson, S. J., Bahrmann, C. P., Shupe, M., DeMott, P. J., Heymsfield, A., and Schofield, R.: The mixed-phase Arctic cloud experiment, Bull. Amer. Meteor. Soc., 88, 205–221, doi:10.1175/BAMS-88-2-205, 2007.

Verlinden, K. L., Thompson, D. W. J., and Stephens, G. L.: The Three-Dimensional Distribution of Clouds over the Southern Hemisphere High Latitudes, J. Climate, 24, 5799–5811, doi:10.1175/2011JCLI3922.1, 2011.

Walsh, J. E., Chapman, W. L., and Portis, D. H.: Arctic cloud fraction and radiative fluxes in atmospheric reanalyses, J. Climate, 22, 2316–2334, doi:10.1175/2008JCLI2213.1, 2009.

Wang, X. and Key, J. R.: Recent trends in Arctic surface, cloud, and radiation properties from space, Science, 299, 1725–1728, 2003.

Wang, X. and Key, J. R.: Arctic surface, cloud, and radiation properties based on the AVHRR Polar Pathfinder dataset. Part I: Spatial and temporal characteristics, J. Climate, 18, 2558–2574, 2005.

Wesslen, C., Tjernström, M., Bromwich, D. H., de Boer, G., Ekman, A. M. L., Bai, L. S., and Wang, S. H.: The Arctic summer atmosphere: an evaluation of reanalyses using ASCOS data, Atmos. Chem. Phys., 14, 2605–2624, doi:10.5194/acp-14-2605-2014, 2014.

Atmos. Meas. Tech. Discuss., doi:10.5194/amt-2016-49, 2016
Manuscript under review for journal Atmos. Meas. Tech.
Published: 7 March 2016

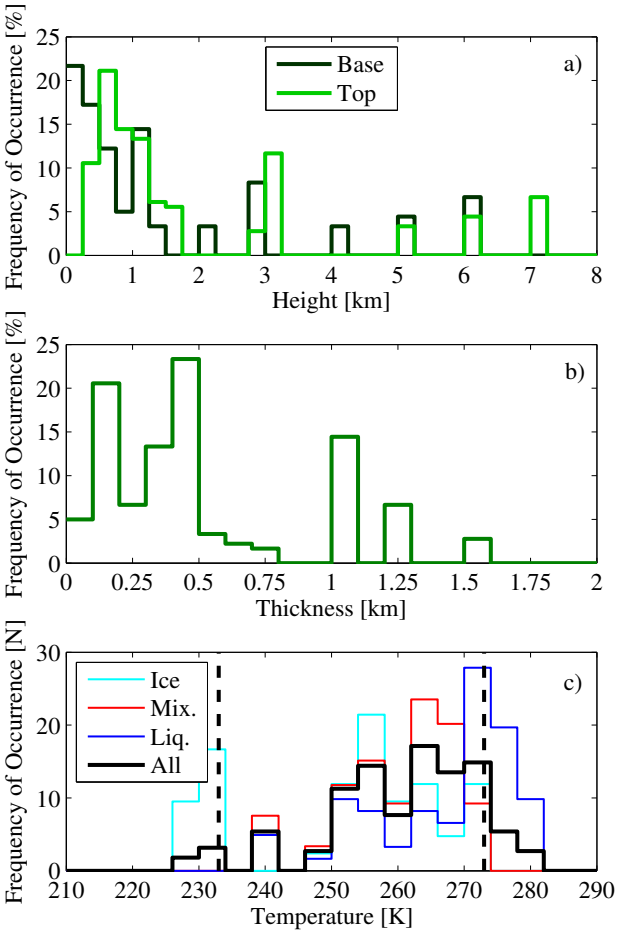

Figure 1. Distributions of macrophysical properties for 222 simulated clouds. a) cloud base height (black) and cloud top height (green), b) physical thickness, and c) cloud temperature. The vertical lines in (c) represent the physical limits imposed on the cloud phase; the lower limit is for liquid, while the upper limit is for ice.

Atmos. Meas. Tech. Discuss., doi:10.5194/amt-2016-49, 2016
Manuscript under review for journal Atmos. Meas. Tech.
Published: 7 March 2016

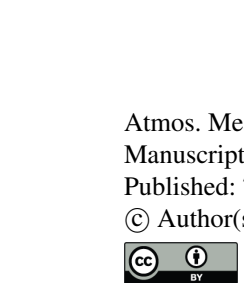

Atmospheric Measurement Techniques Discussions

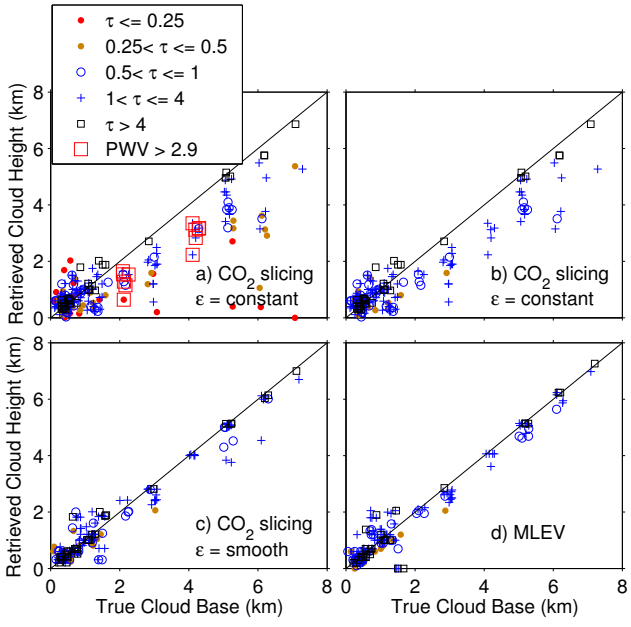

Figure 2. Retrieved versus true cloud base for cases with no error and a simulated instrument resolution of 0.5 cm^{-1}. In a) and c), "CO_2 slicing" refers to the CO_2 slicing/sorting method. The CO_2 slicing/sorting method and MLEV methods are described in the text.

Atmos. Meas. Tech. Discuss., doi:10.5194/amt-2016-49, 2016
Manuscript under review for journal Atmos. Meas. Tech.
Published: 7 March 2016

Atmospheric Measurement Techniques Discussions

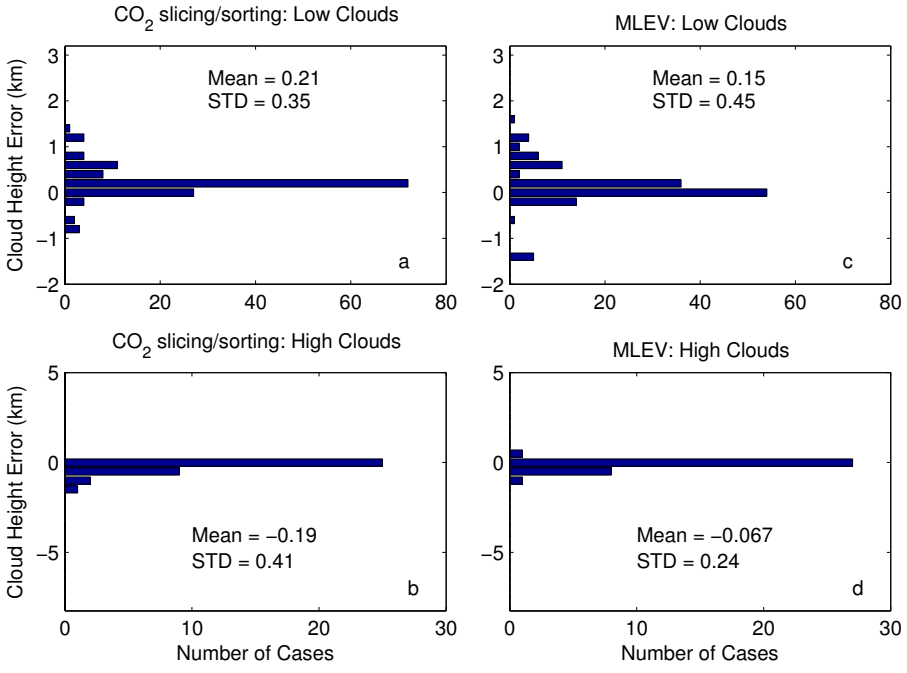

Figure 3. Errors in cloud heights retrieved from infrared downwelling radiances (at an instrument resolution of 0.5 cm^{-1}) for single-layer model clouds with no errors imposed. The retrieval methods are given in the titles. Low clouds are defined to have bases below 2 km while high clouds have bases $\geq$ 2 km.

Atmos. Meas. Tech. Discuss., doi:10.5194/amt-2016-49, 2016
Manuscript under review for journal Atmos. Meas. Tech.
Published: 7 March 2016

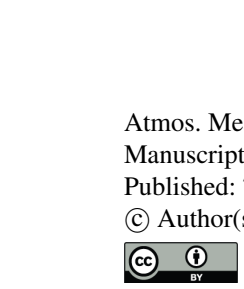

Atmospheric Measurement Techniques Discussions

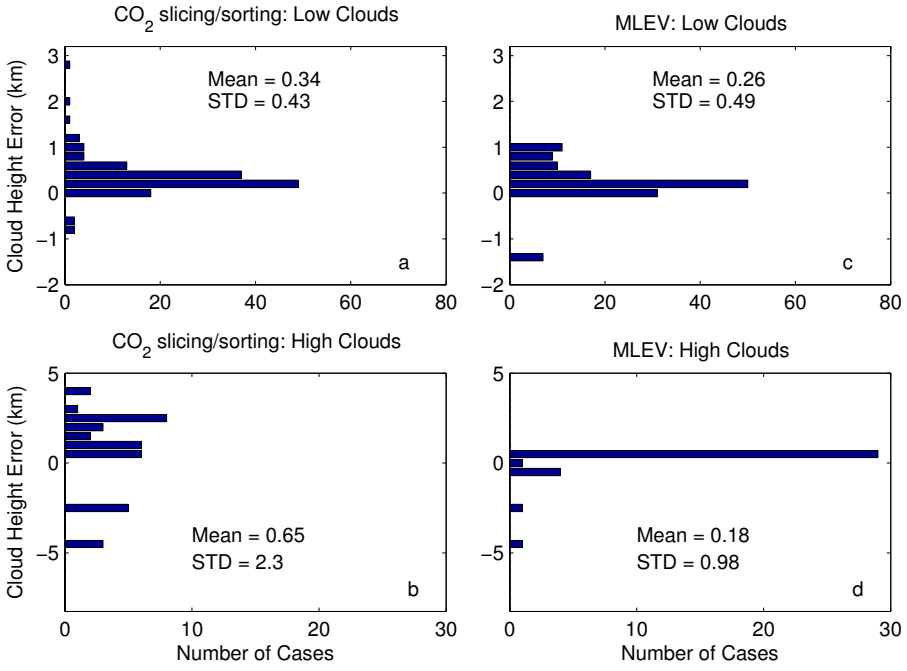

Figure 4. Errors in cloud heights retrieved from infrared downwelling radiances (at an instrument resolution of 0.5 cm^{-1}) for single-layer model clouds with positive biases in the temperature profile used for the retrieval (0.2 K at all heights) for a) low clouds (cloud bases < 2 km) retrieved using CO_2 slicing/sorting, b) low clouds retrieved using MLEV, c) High clouds (defined to have bases $\geq$ 2 km) retrieved using CO_2 slicing/sorting, and d) high clouds retrieved using MLEV.

Atmos. Meas. Tech. Discuss., doi:10.5194/amt-2016-49, 2016
Manuscript under review for journal Atmos. Meas. Tech.
Published: 7 March 2016

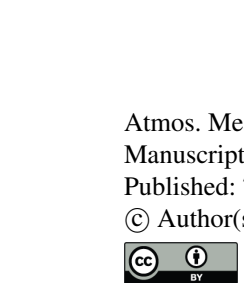

Atmospheric Measurement Techniques Discussions

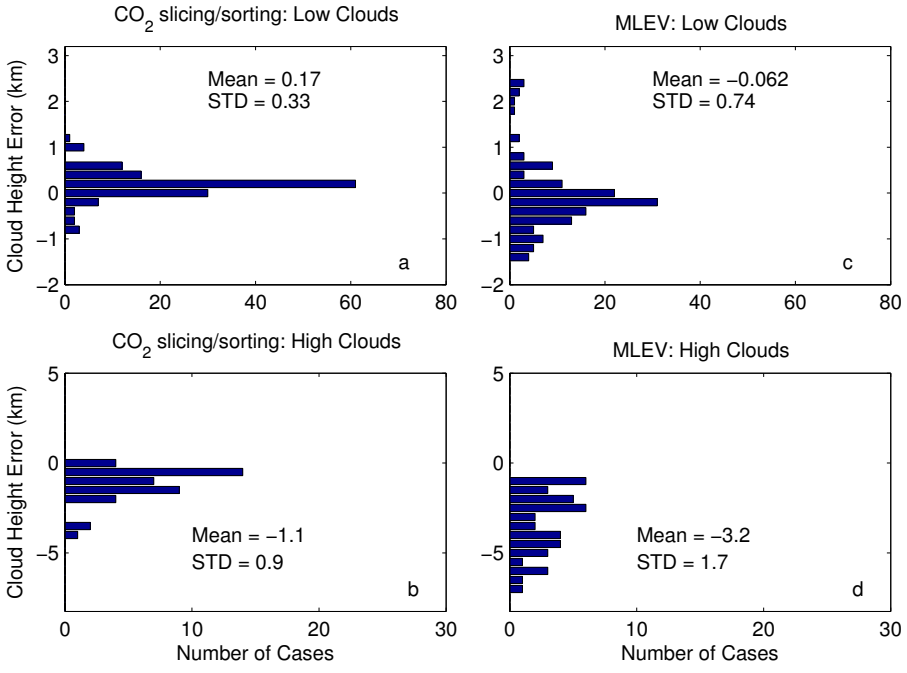

Figure 5. Errors in cloud heights retrieved from infrared downwelling radiances (at an instrument resolution of 0.5 cm^{-1}) for single-layer model clouds with negative biases imposed on the water vapor profile used in the retrieval (of 10% at all heights) for a) low clouds (cloud bases < 2 km) retrieved using CO_2 slicing/sorting, b) low clouds retrieved using MLEV, and c) high clouds (defined to have bases $\geq$ 2 km) retrieved using CO_2 slicing/sorting, and d) high clouds retrieved using MLEV.

Atmos. Meas. Tech. Discuss., doi:10.5194/amt-2016-49, 2016
Manuscript under review for journal Atmos. Meas. Tech.
Published: 7 March 2016

Atmospheric Measurement Techniques Discussions

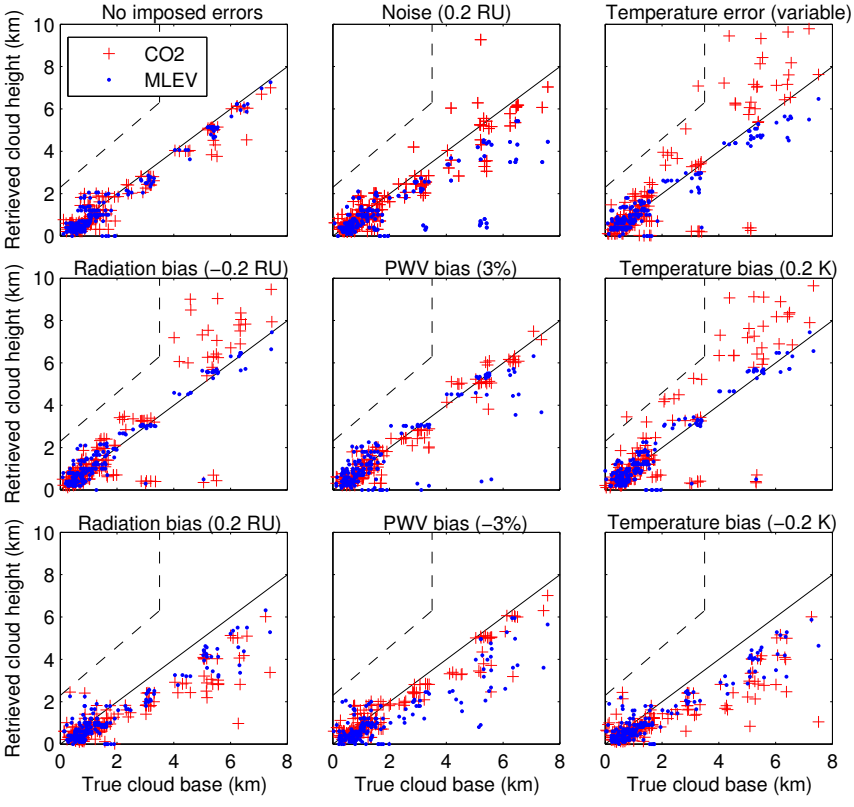

Figure 6. Retrieved versus true cloud base for cases with the errors shown in the titles for the CO_2 slicing/sorting (CO2) and MLEV methods (at a resolution of 0.5 cm^{-1}). The dashed lines indicate the upper left region where points rarely lie.

Atmos. Meas. Tech. Discuss., doi:10.5194/amt-2016-49, 2016
Manuscript under review for journal Atmos. Meas. Tech.
Published: 7 March 2016

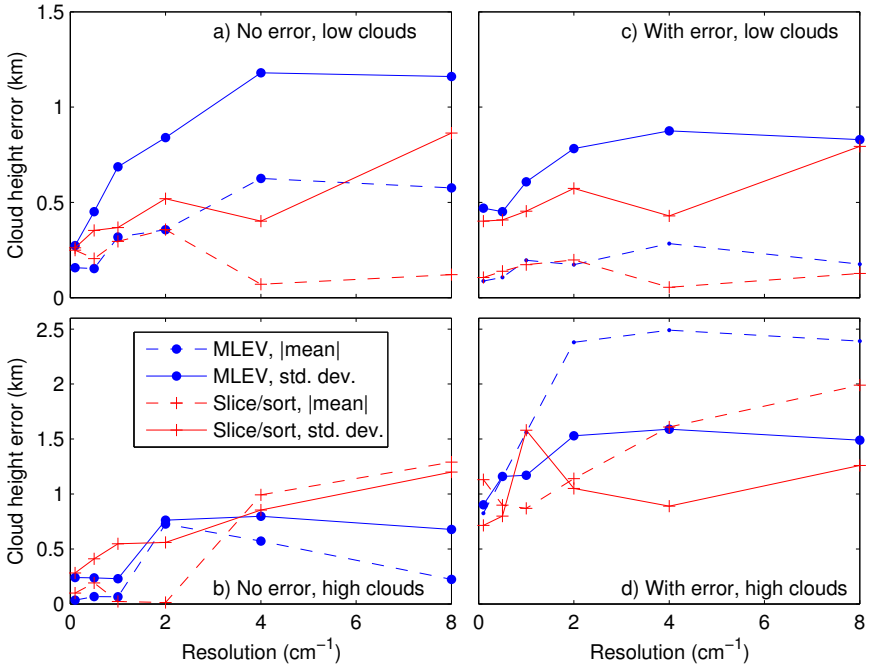

Figure 7. Absolute value of mean error in retrieved cloud heights and standard deviation in retrieved cloud heights as a function of instrument resolution for a) low clouds (cloud bases below 2 km) with no imposed error, b) high clouds (bases of 2 km and above) with no imposed error, c) low clouds with imposed error, and d) high clouds with imposed error. The errors imposed are 0.1 mW / (m^2 sr cm^{-1}) noise in the cloudy-sky radiance and a bias of -0.1 K in the temperature profile used for the retrieval. One outlier (with a cloud base at 0.3 km and a retrieved cloud base of 8 km) was removed from the set of retrievals at 0.1 cm^{-1} with imposed error.

Atmos. Meas. Tech. Discuss., doi:10.5194/amt-2016-49, 2016
Manuscript under review for journal Atmos. Meas. Tech.
Published: 7 March 2016

Atmospheric Measurement Techniques Discussions

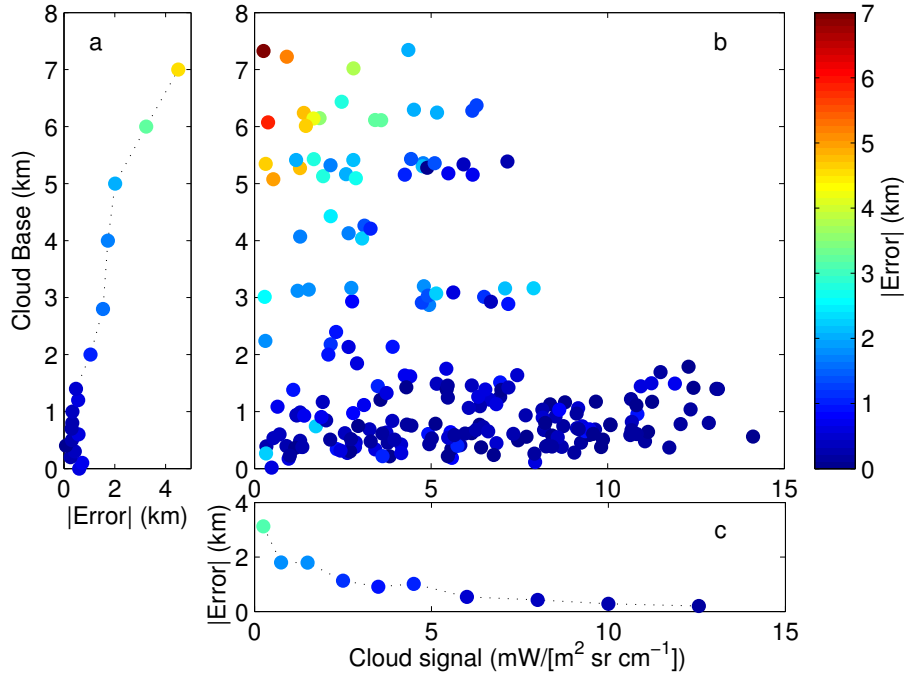

Figure 8. (a) Absolute value of binned mean error in retrieved cloud heights (x-axis) as a function of cloud base height (y-axis). (b) Absolute value of cloud height error (given in colorbar) as a function of cloud base height and cloud signal (root-mean-square of cloudy - clear sky radiance). A small random number is added to each cloud base height in this panel to make them more easily distinguishable. (c) Absolute value of binned mean error as a function of cloud signal. Cloud heights were retrieved using CO_2 slicing/sorting from downwelling radiances at a resolution of 4 cm^{-1}. Noise of 0.1 mW/(m^2 sr cm^{-1}) was added to the cloudy-sky radiance and a bias of -0.1 K was added to the temperature profile used in the retrieval.

Atmos. Meas. Tech. Discuss., doi:10.5194/amt-2016-49, 2016
Manuscript under review for journal Atmos. Meas. Tech.
Published: 7 March 2016

Atmospheric Measurement Techniques Discussions

Table 1. Errors in retrieved cloud height (retrieved height - true cloud base) for clouds with bases below 2 km using the CO_2 slicing/sorting and MLEV retrieval methods at a resolution of 0.5 cm^{-1}. Errors were determined by imposing a source of error (Source) on either the cloudy-sky radiance: noise or radiation bias (Bias) or on the simulated radiances used in the retrieval: temperature, humidity or CO_2 profiles used in the retrieval. For profiles, biases were imposed at all heights, except for variable temperature errors (var.). The mean error (Mean) and the standard deviation of the errors in retrieved cloud height (STD) are given. There were 165 cases, of which some were omitted based on screening (Omit.). The final row shows an estimate of the combined error for realistic sources of errors, calculated as described in the text.

		CO_2 slicing/sorting			MLEV		
Source	Value	Mean (km)	STD (km)	Omit. (#)	Mean (km)	STD (km)	Omit. (#)
None	-	0.21	0.35	21	0.15	0.45	22
Noise	0.2	0.25	0.42	22	0.13	0.45	21
Bias (RU)	0.2	0.05	0.40	19	0.09	0.49	19
Bias (RU)	-0.2	0.31	0.34	22	0.36	0.40	22
Temp. (K)	0.2	0.34	0.43	22	0.26	0.49	22
Temp. (K)	-0.2	0.05	0.38	19	0.05	0.48	19
Temp. (K)	var.	0.27	0.40	21	0.25	0.46	21
W.V. (%)	3	0.23	0.33	21	0.28	0.55	21
W.V. (%)	3	0.21	0.36	19	0.04	0.52	19
W.V. (%)	10	0.21	0.35	25	0.27	0.64	26
W.V. (%)	10	0.17	0.33	19	-0.06	0.74	19
CO_2 (%)	0.5	0.25	0.34	21	0.17	0.47	21
CO_2 (%)	0.5	0.20	0.37	18	0.15	0.45	18
Total	-	0.2	0.5	-	0.2	0.6	-

Atmos. Meas. Tech. Discuss., doi:10.5194/amt-2016-49, 2016
Manuscript under review for journal Atmos. Meas. Tech.
Published: 7 March 2016

Atmospheric Measurement Techniques Discussions

Table 2. Errors in retrieved cloud height (retrieved height - true cloud base) for clouds with bases $\geq$ 2 km using the CO_2 slicing/sorting and MLEV retrieval methods at a resolution of 0.5 cm^{-1}. Errors were determined by imposing a source of error (Source) on either the cloudy-sky radiance: noise or radiation bias (Bias) or on the simulated radiances used in the retrieval: temperature, humidity or CO_2 profiles used in the retrieval. For profiles, biases were imposed at all heights, except for variable temperature errors (var.). The mean error (Mean) and the standard deviation of the errors in retrieved cloud height (STD) are given. There were 67 cases, of which some were omitted based on screening (Omit.). The final row shows an estimate of the combined error for realistic sources of errors, calculated as described in the text.

		CO_2 slicing/sorting			MLEV		
Source	Value	Mean (km)	STD (km)	Omit. (#)	Mean (km)	STD (km)	Omit. (#)
None	-	-0.19	0.41	28	-0.07	0.24	28
Noise	0.2	-0.25	1.30	27	-1.72	1.45	28
Bias (RU)	0.2	-1.47	0.99	27	-0.91	0.57	27
Bias (RU)	-0.2	0.49	1.98	29	0.13	0.64	27
Temp. (K)	0.2	0.65	2.35	29	0.18	0.98	29
Temp. (K)	-0.2	-1.67	1.15	27	-1.08	0.64	27
Temp. (K)	var.	0.51	2.38	28	-0.39	0.57	28
W.V. (%)	3	0.02	0.46	29	-0.64	1.44	29
W.V. (%)	3	-0.42	0.72	27	-1.34	1.12	27
W.V. (%)	10	0.51	0.84	29	-2.90	1.81	29
W.V. (%)	10	-1.09	0.90	24	-3.23	1.74	24
CO_2 (%)	0.5	0.06	0.49	29	0.15	0.25	36
CO_2 (%)	0.5	0.44	0.52	27	-0.30	0.37	27
Total	-	-1.7	2.0	-	-2.4	1.7	-